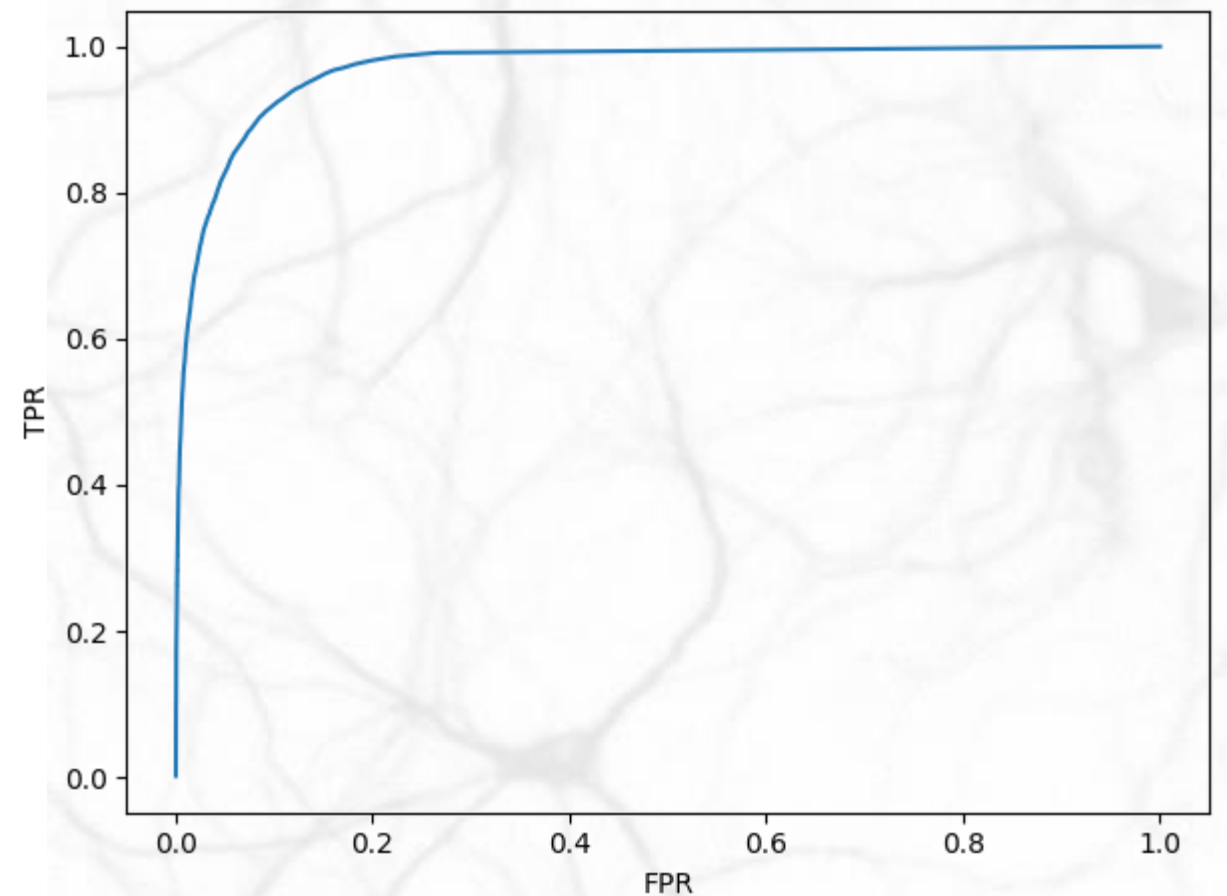
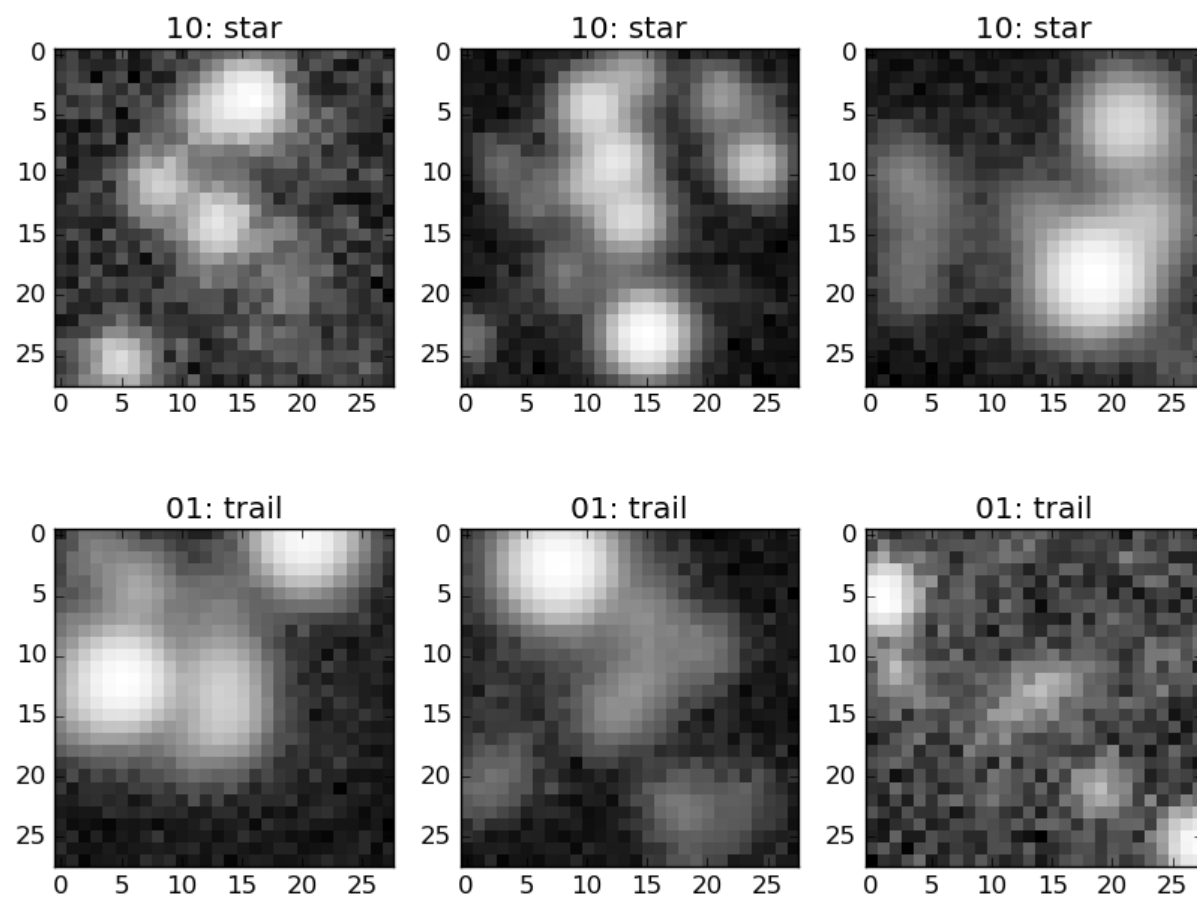


Inferring from astronomical images using Deep Learning

Emmanuel Bertin (IAP)

A typical astronomical image analysis problem

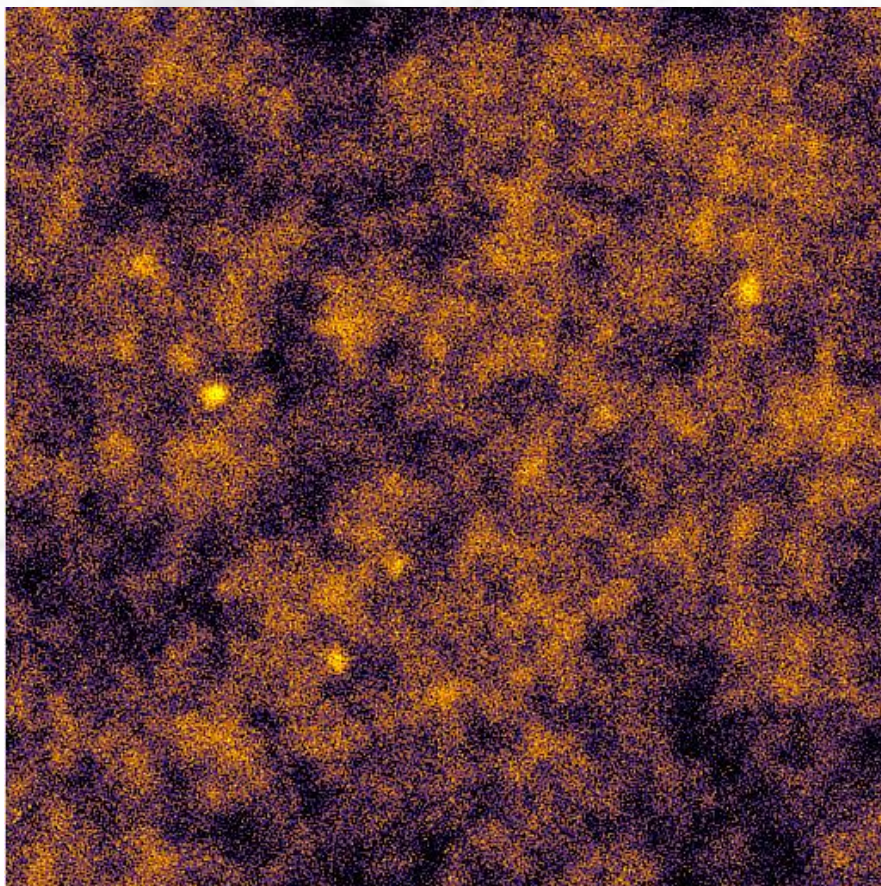
- Example: Identify a specific type of source in a crowded field



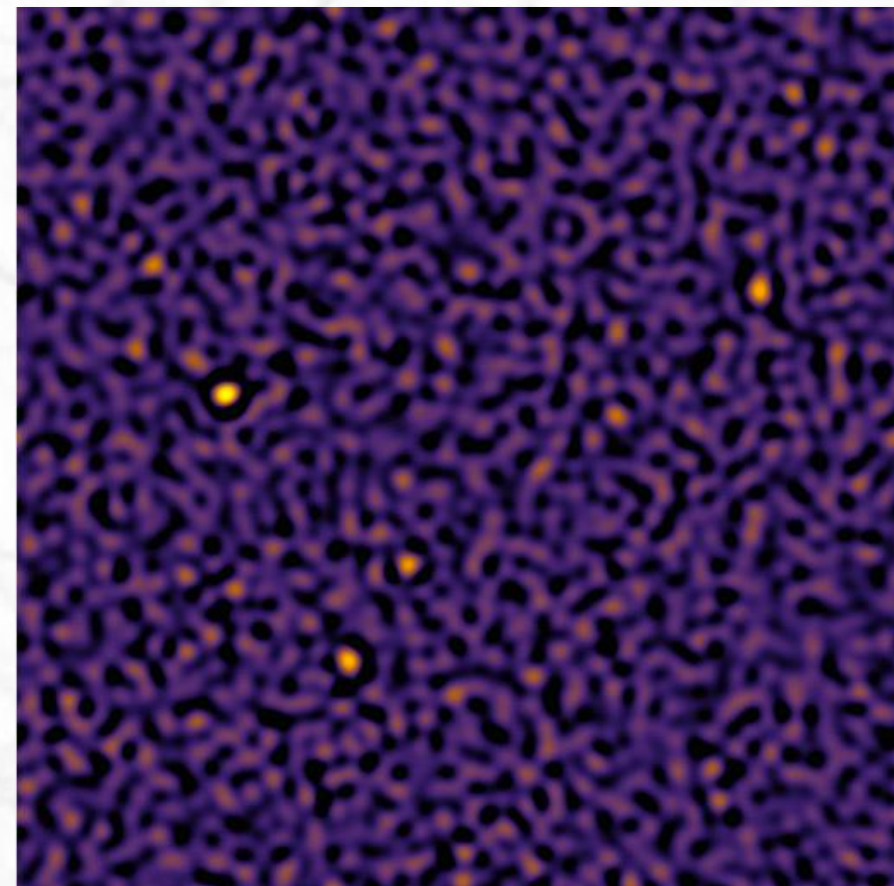
- We want probabilities!

Matched filter

- Optimal linear filter for identifying a known pattern with added wide-sense stationary noise: $H(\mathbf{k}) = \frac{\Phi^*(\mathbf{k})}{P(\mathbf{k})}$
- Convolve with $h(\mathbf{x}) = \phi^\top(\mathbf{x})$ for white noise
- Deconvolve with $\phi(\mathbf{x})$ for confusion noise

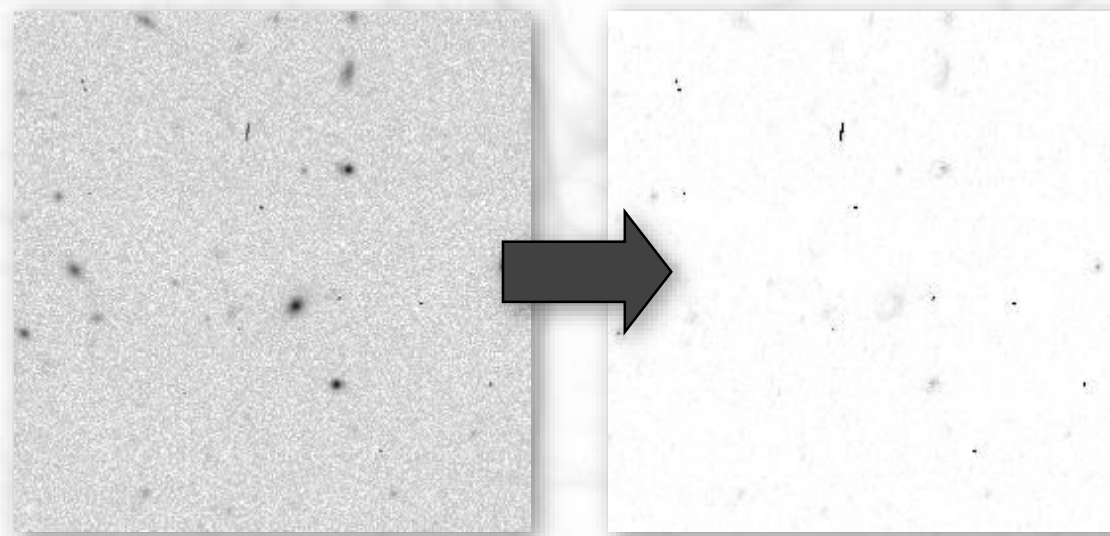
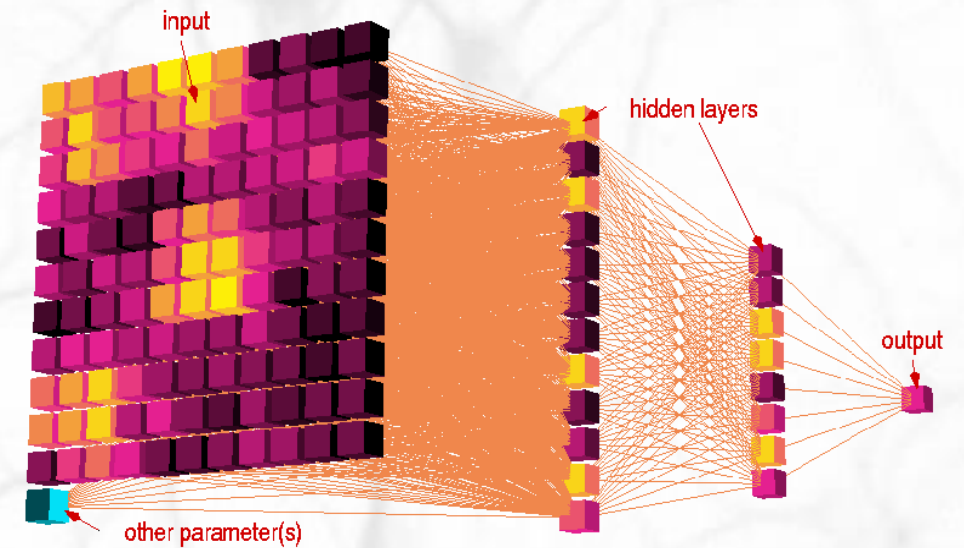


→
filtered

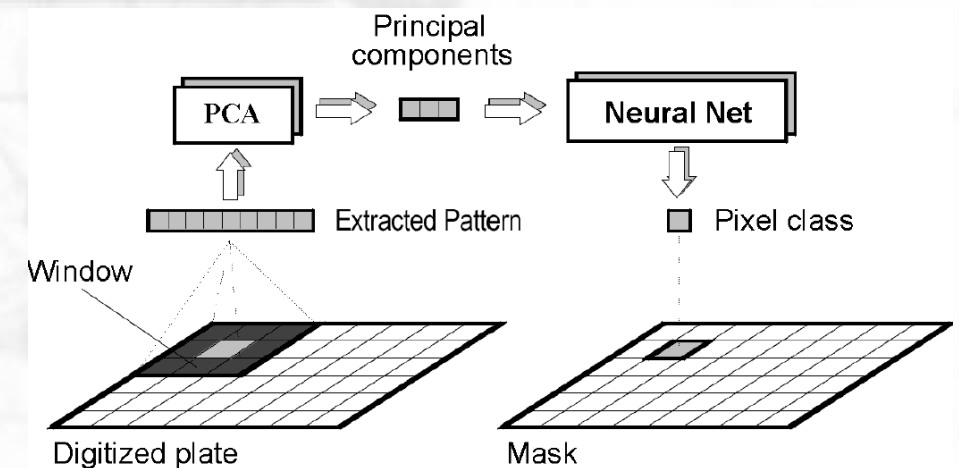


Early AI-driven detection filters

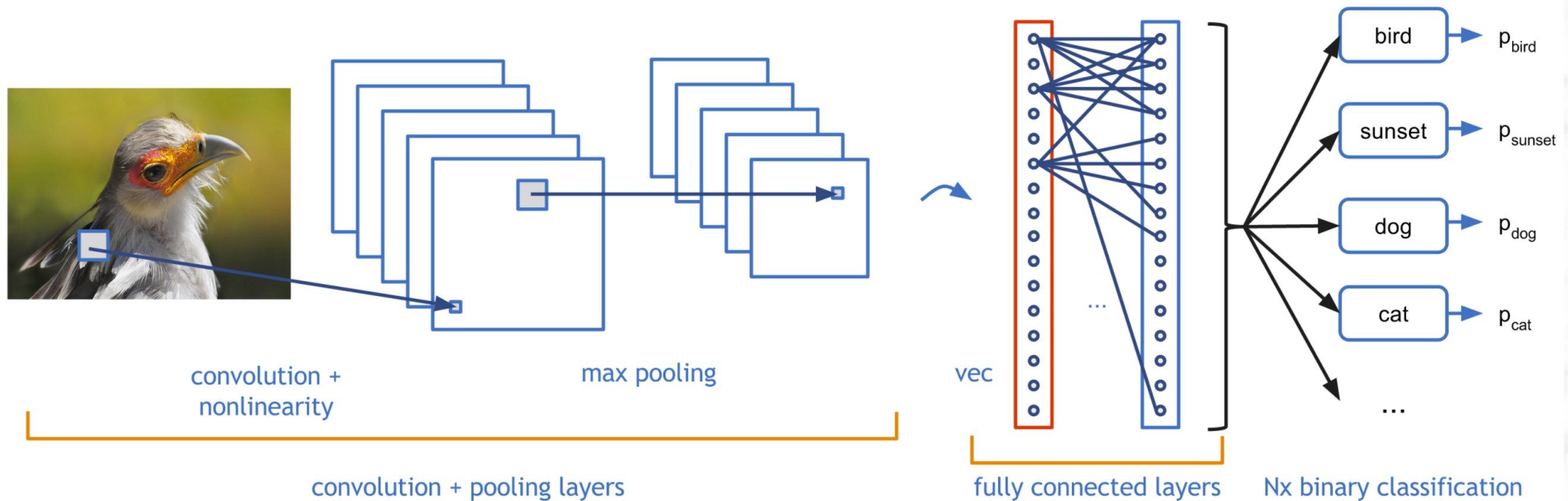
- “EyE” (1998, 2001)
 - Multilayered Perceptron where inputs are compressed pixel values
 - Used in production for detecting CR impacts



- “NExtractor (Andreon et al. 2000)
 - PCA + multilayered Perceptron

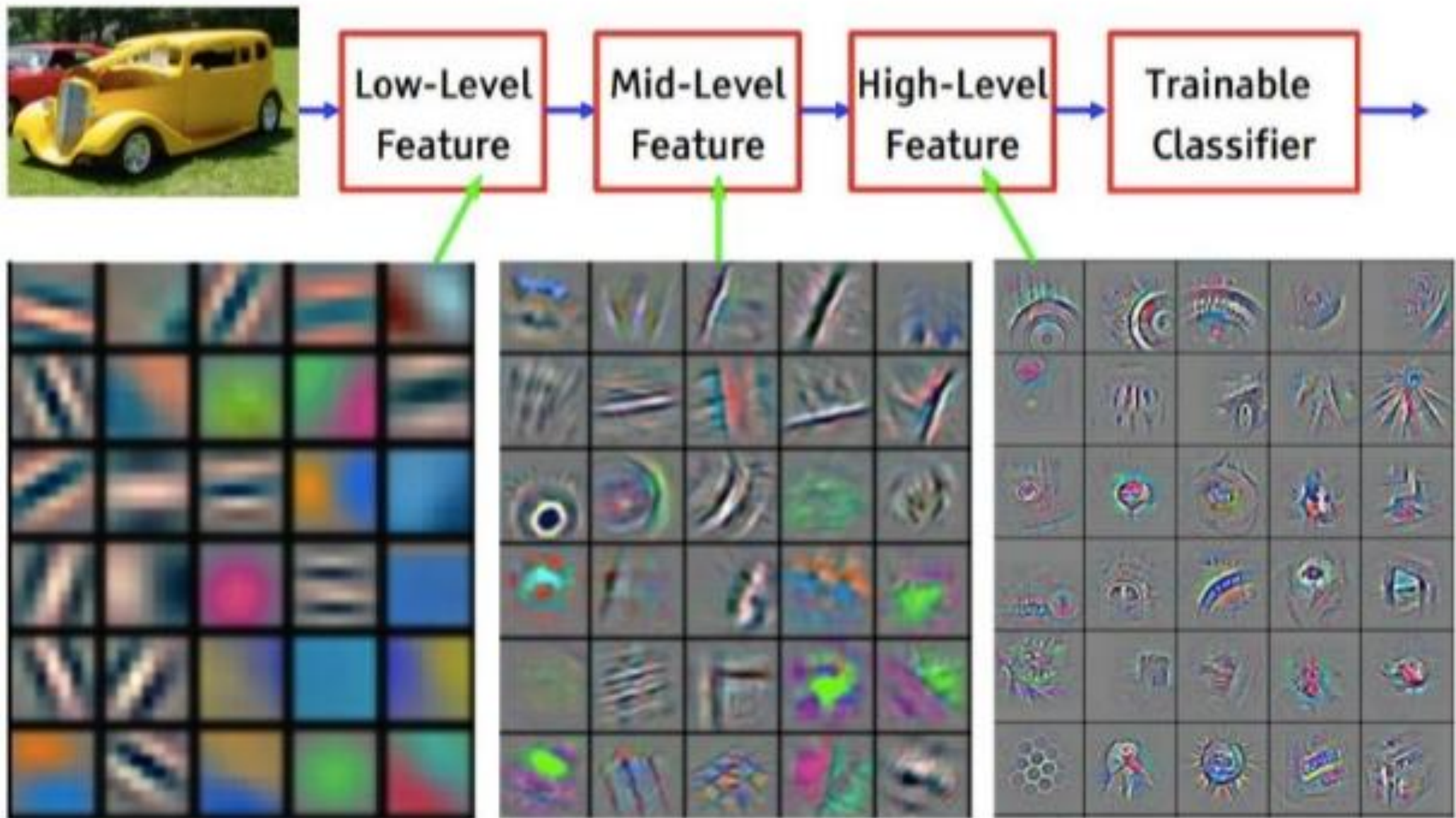


Deep Learning with convolutional layers



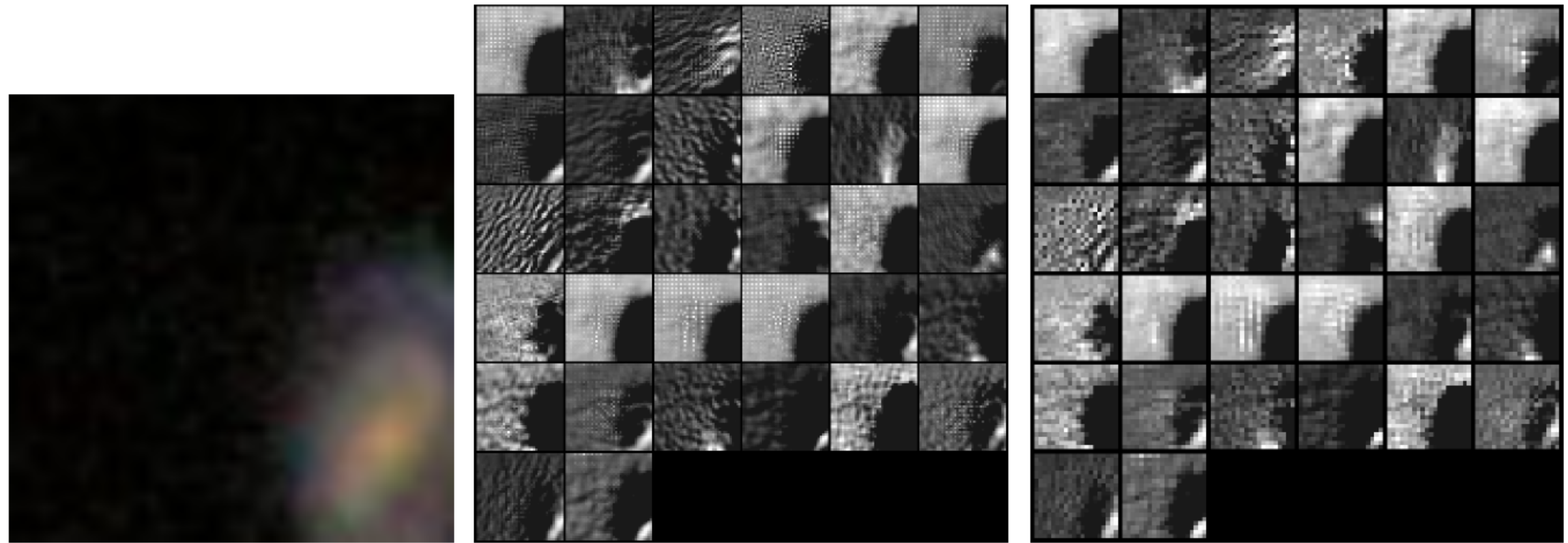
- Convergence of several breakthroughs
 - Convolutional nets (CNNs, e.g., [LeCun et al. 1998](#))
 - “Guided” unsupervised learning on individual layers (e.g., [Hinton et al. 2006](#))
 - Learning of sparse representations (e.g., [Ranzato et al. 2007](#))
 - GPU libraries (e.g., cuDNN) 
 - Availability of large datasets with labels throughout the web (e.g. ImageNet)
- Research funding by GAFAs motivated by the monetization of big data

Hierarchy of representations



Feature visualization of convolutional net trained on ImageNet from [Zeiler & Fergus 2013]

Application to the Kaggle Galaxy Challenge (Dieleman et al. 2015)



input (45×45)

layer 1 (32 maps, 40×40)

pooling 1 (32 maps, 20×20)



layer 2
(64 maps, 16×16)

pooling 2
(64 maps, 8×8)

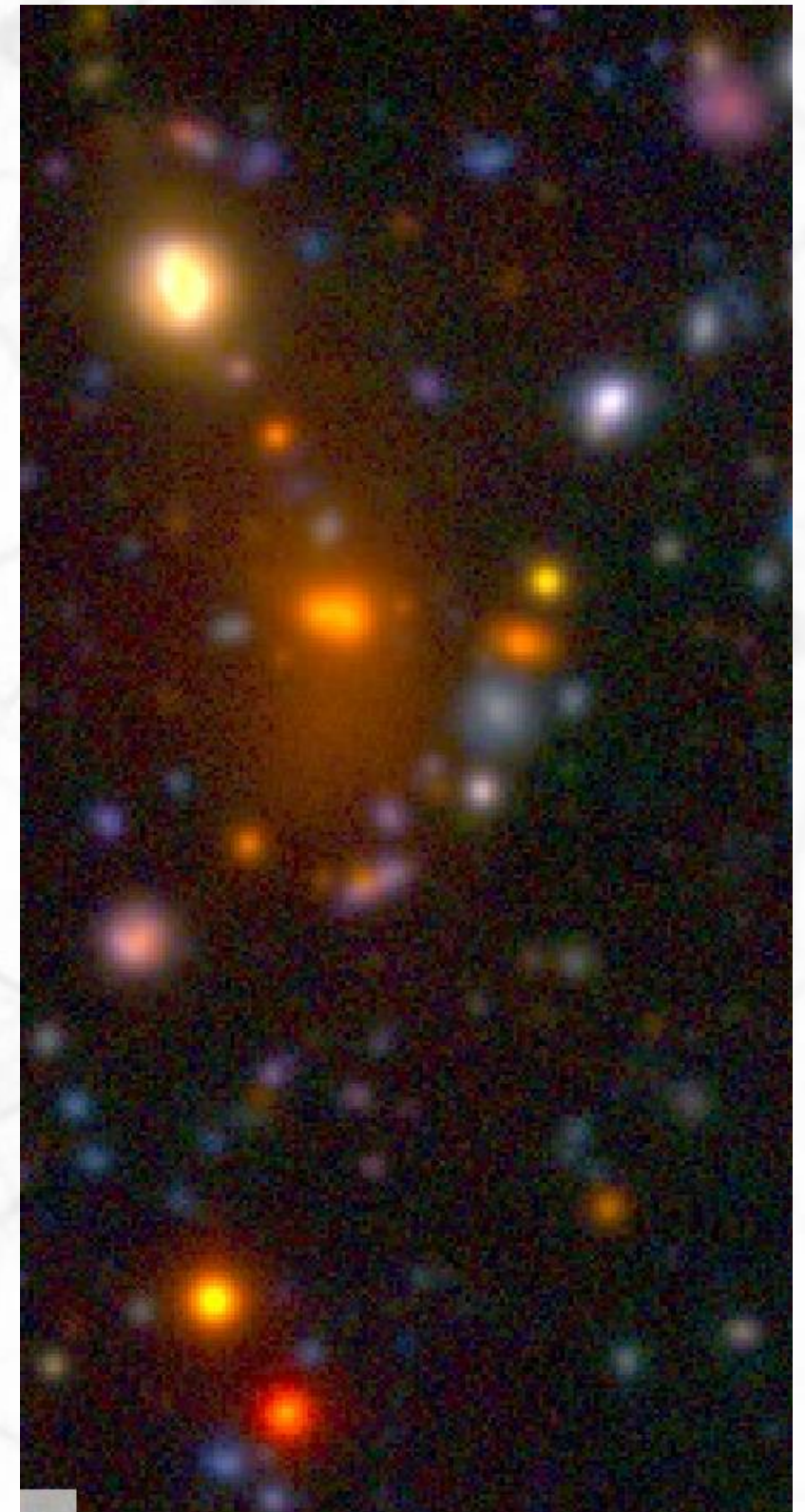
layer 3
(128 maps, 6×6)

layer 4
(128 maps, 4×4)

pooling 4
(128 maps, 2×2)

Training with astronomical images

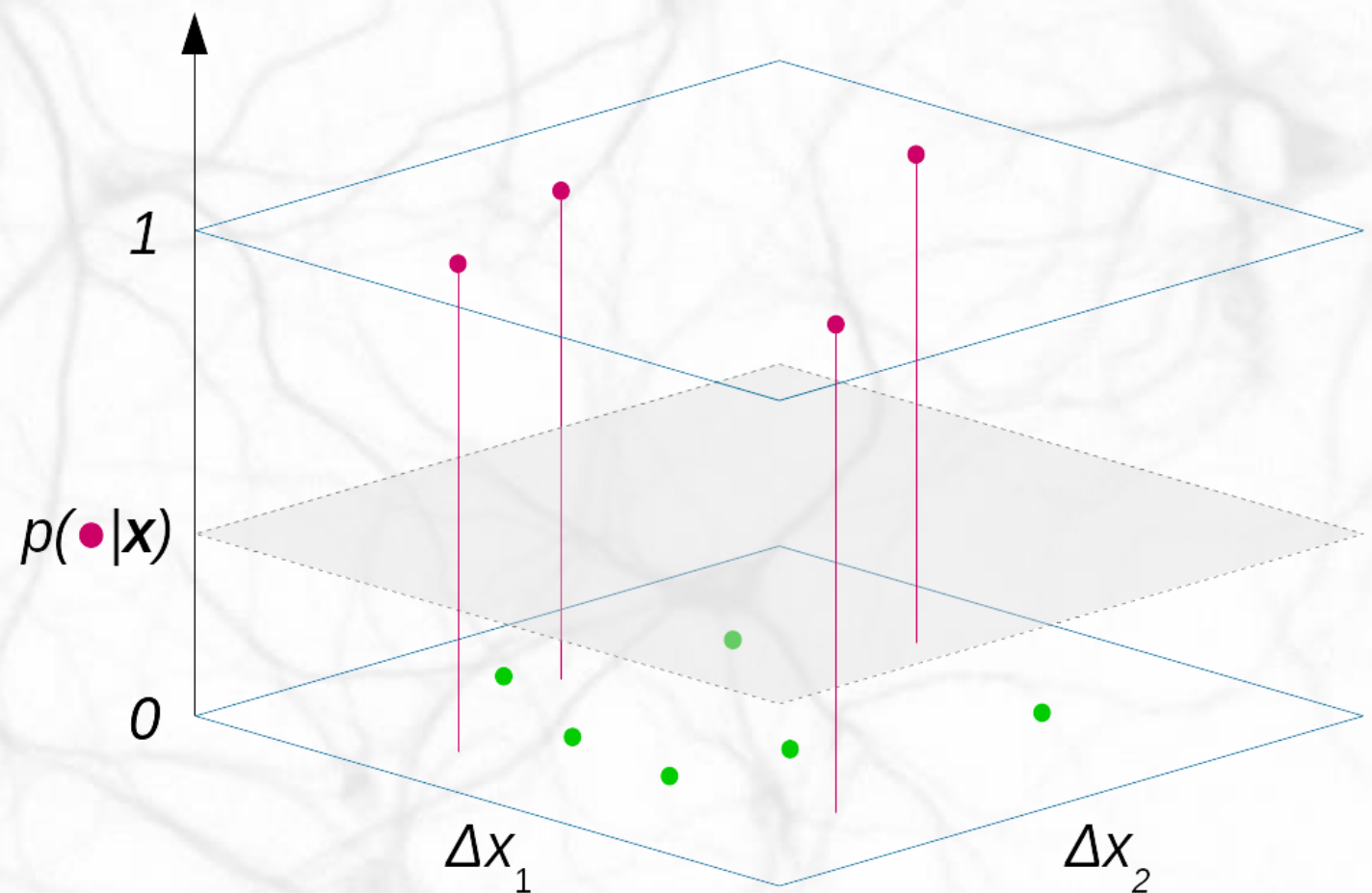
- Deep sky images:
 - Multispectral data are now commonplace
 - Lighting and projection effects not dominant
 - Fuzzy and noisy (SNR \sim 1)
 - Spectral distributions and image formation processes (PSF + noise) can generally be accurately modeled
 - Augmented reality is an efficient approach



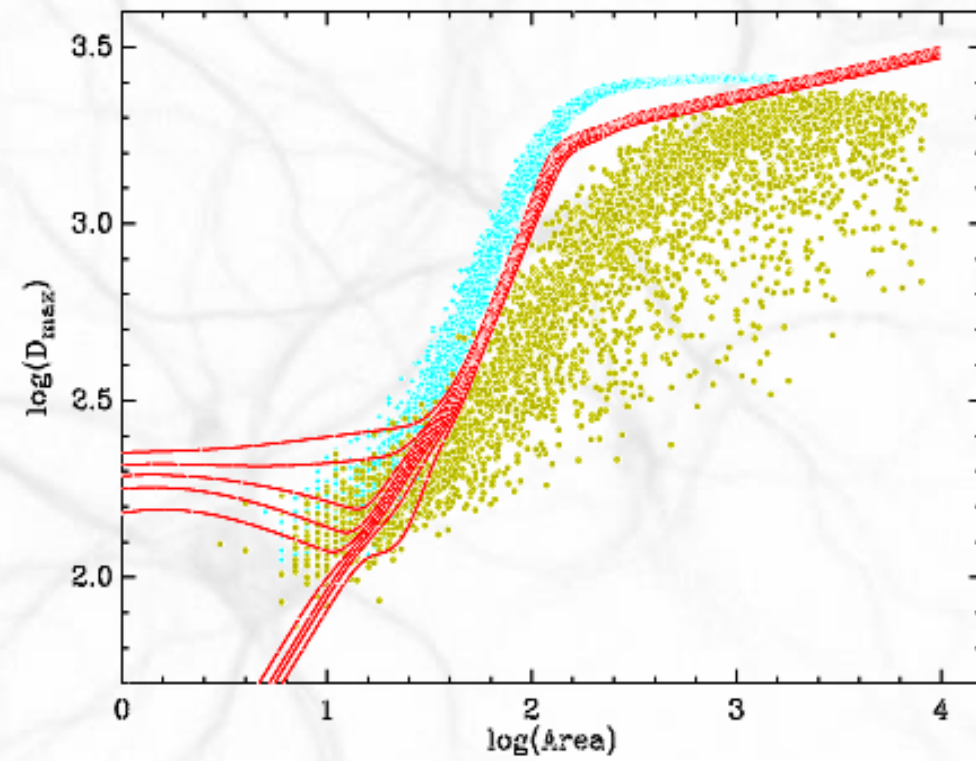
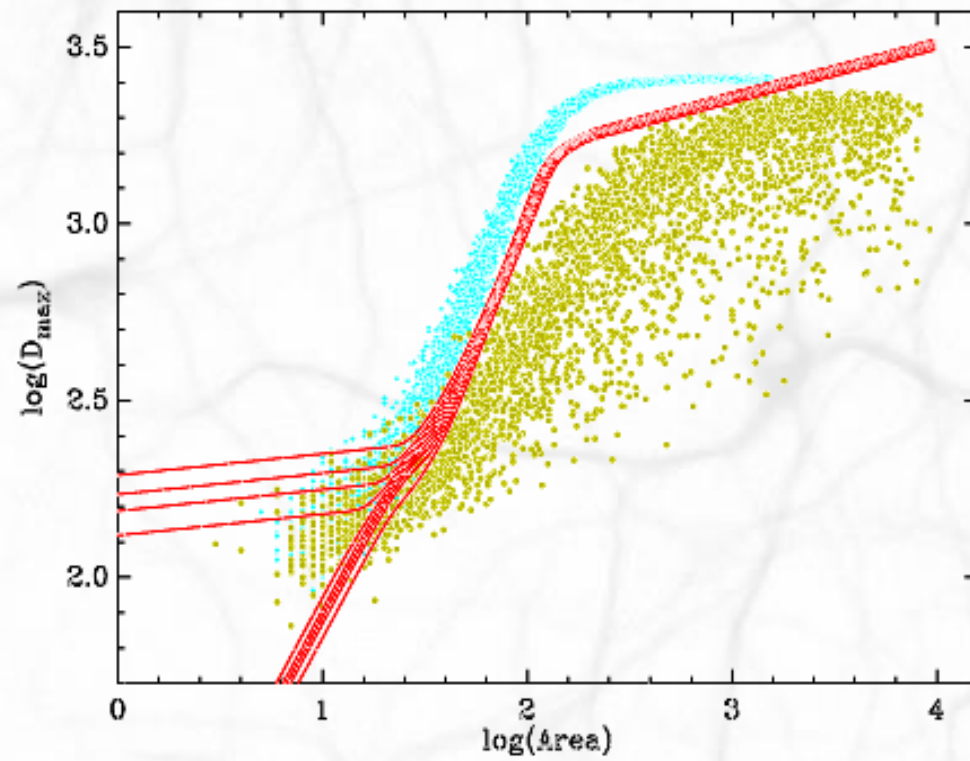
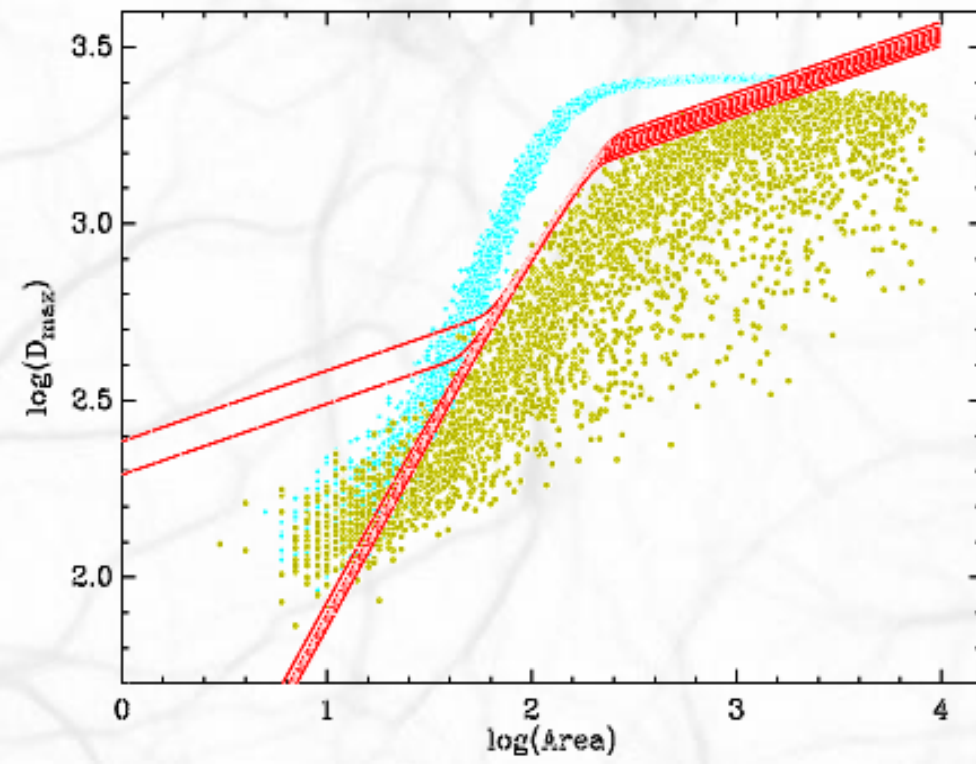
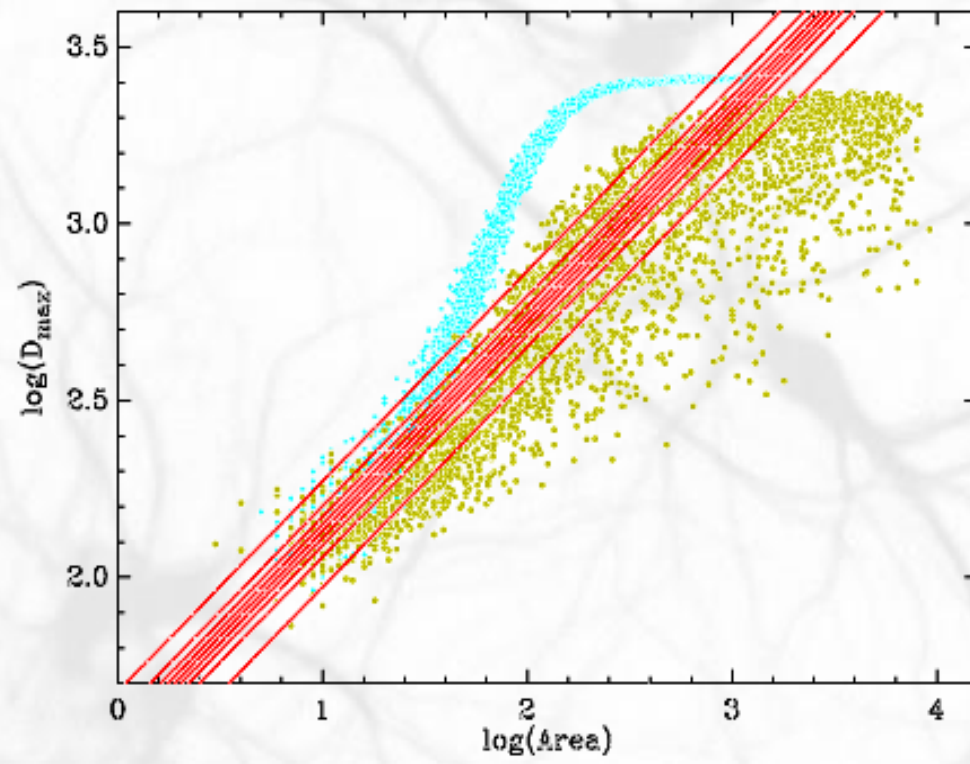
Estimating posterior probabilities

- The output of perfectly trained neural network classifiers can provide direct estimation of the posterior class probabilities (**Pearlmutter & Hampshire 1990, Richard & Lippmann 1991, Miller et al. 1991, Rojas 1996, ...**)
 - Valid for a large range of cost functions (including quadratic and cross-entropy)
 - Requires a sufficiently powerful model with excellent generalization abilities
 - Both a blessing and a curse!
 - Importance of sample selection for training
 - Strong class imbalance shifts decision boundaries
 - “Hidden” priors

$$P(c_i|\mathbf{x}) = \frac{p(\mathbf{x}|c_i)P(c_i)}{\sum_j p(\mathbf{x}|c_j)P(c_j)}$$

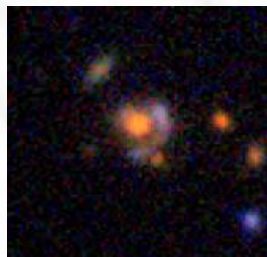


Example

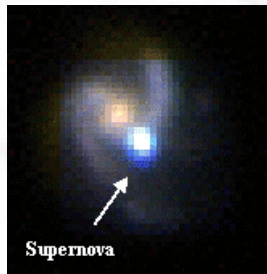


Class imbalance

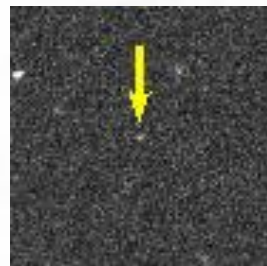
- Class imbalance is often huge in representative samples
 - Interesting objects among regular ones: $P \sim 10^{-6}$ to $\sim 10^{-5}$:



- Strong lenses (Jacobs et al. 2018)



- Galaxies with a detectable SN (Smartt et al. 2018)



- Trans-Neptunian Objects (Gladman et al. 1998)

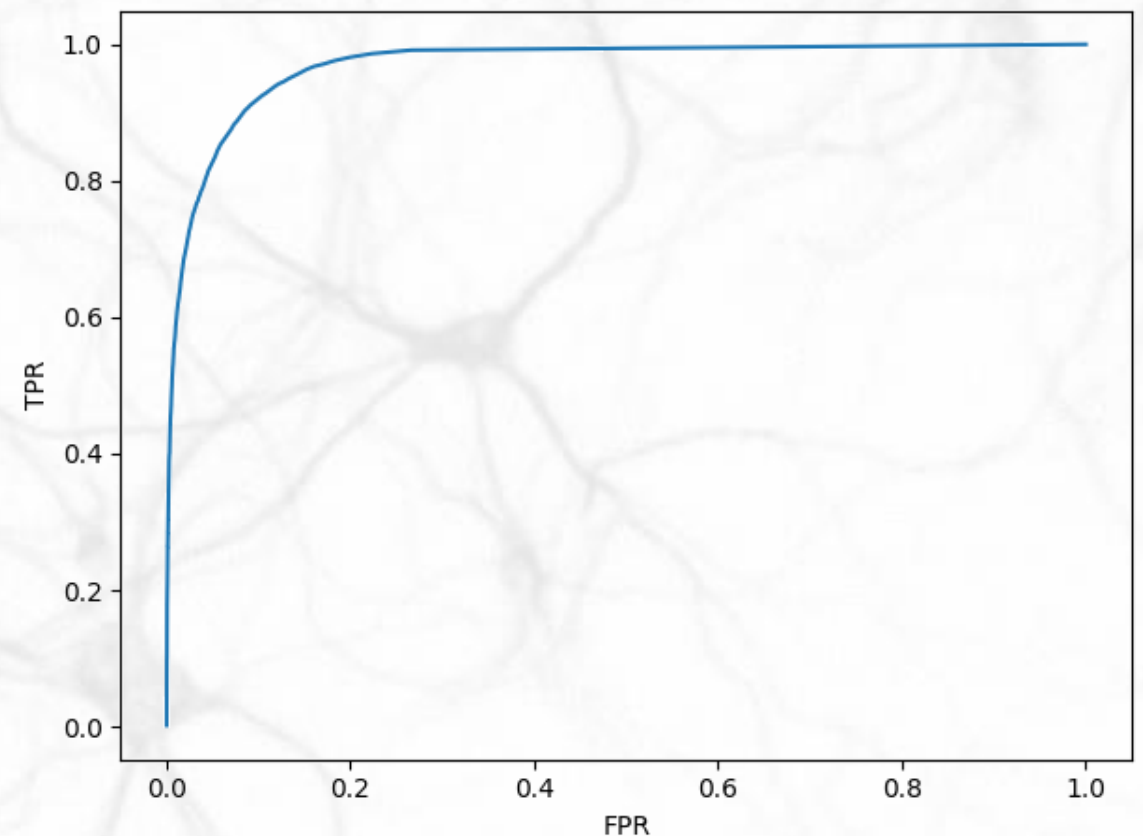
- Even worse when considering blind searches in images: one often has $P \sim 10^{-7}$

Re-balancing training

- Rare events in excess in the training set: $P_T(c)$
- Correct output probabilities using the true prior $P(c)$:

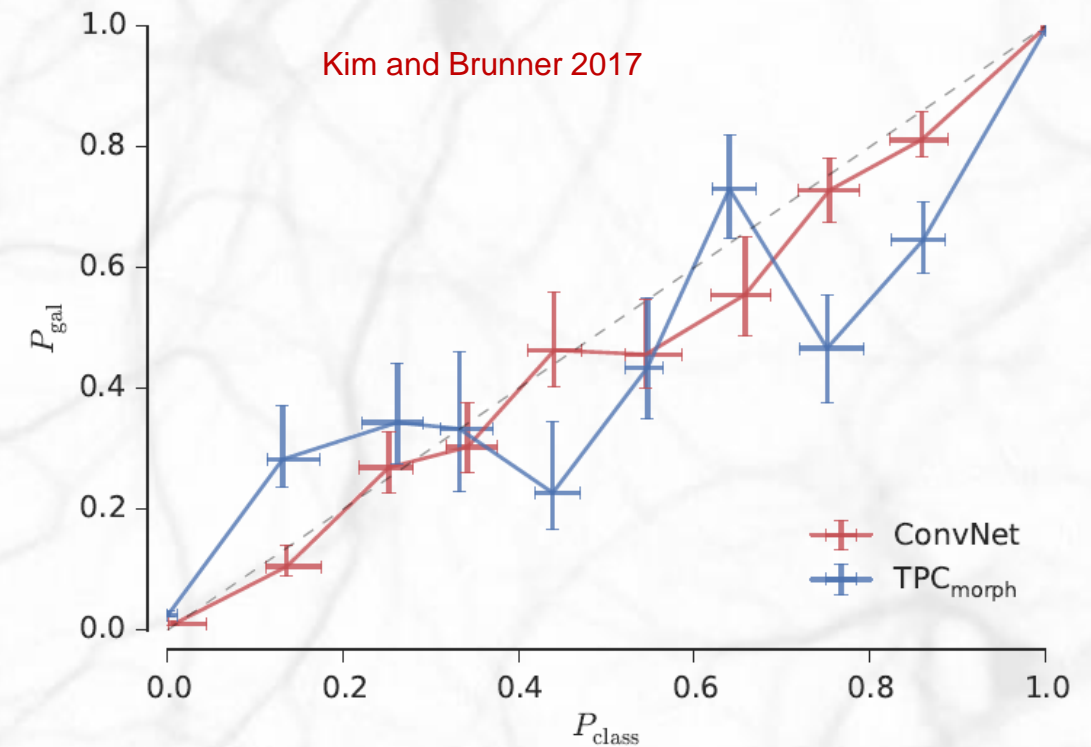
$$P(c|\mathbf{x}) = \frac{P_T(c|\mathbf{x})P(c)}{P_T(c) \sum_{c'} \frac{P(c')}{P_T(c')} P_T(c'|\mathbf{x})}$$

- Works well in good training conditions
(large samples, no mismatch)
- Can be checked on ROC curves
- Or adjust thresholds directly from ROC curves



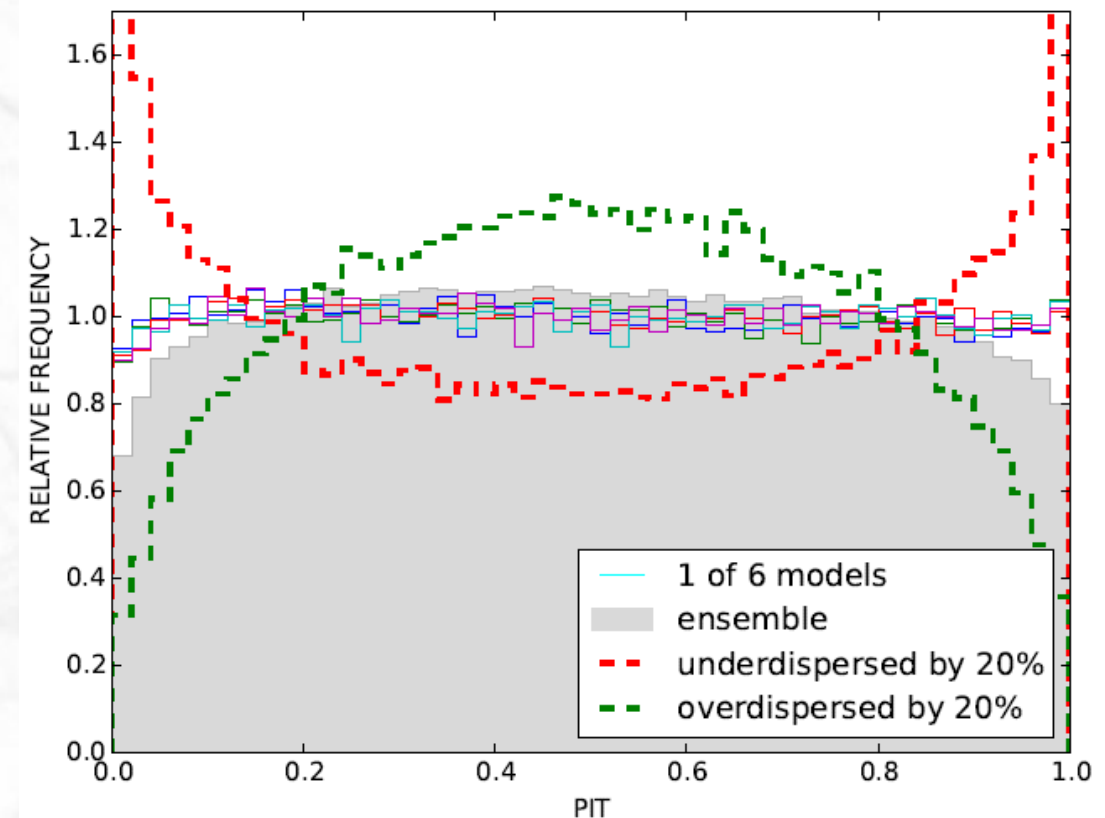
Estimating the accuracy of the posterior probabilities

- Two mutually exclusive classes:
Check TPR in intervals of output $P(c|\mathbf{x})$



- Probability Integral Transform (**Dawid 1984**):

$$PIT(c_i) = \sum_{c_j=c_i} \sum_{c=1}^{c=c_j} P(c|\mathbf{x}_j)$$



Side note: dealing with the high dynamic range

- Most CNNs are meant to operate with images coming straight from JPEG, PNG, TIFF or even MPG files were the recorded pixel values are “gamma-compressed”:

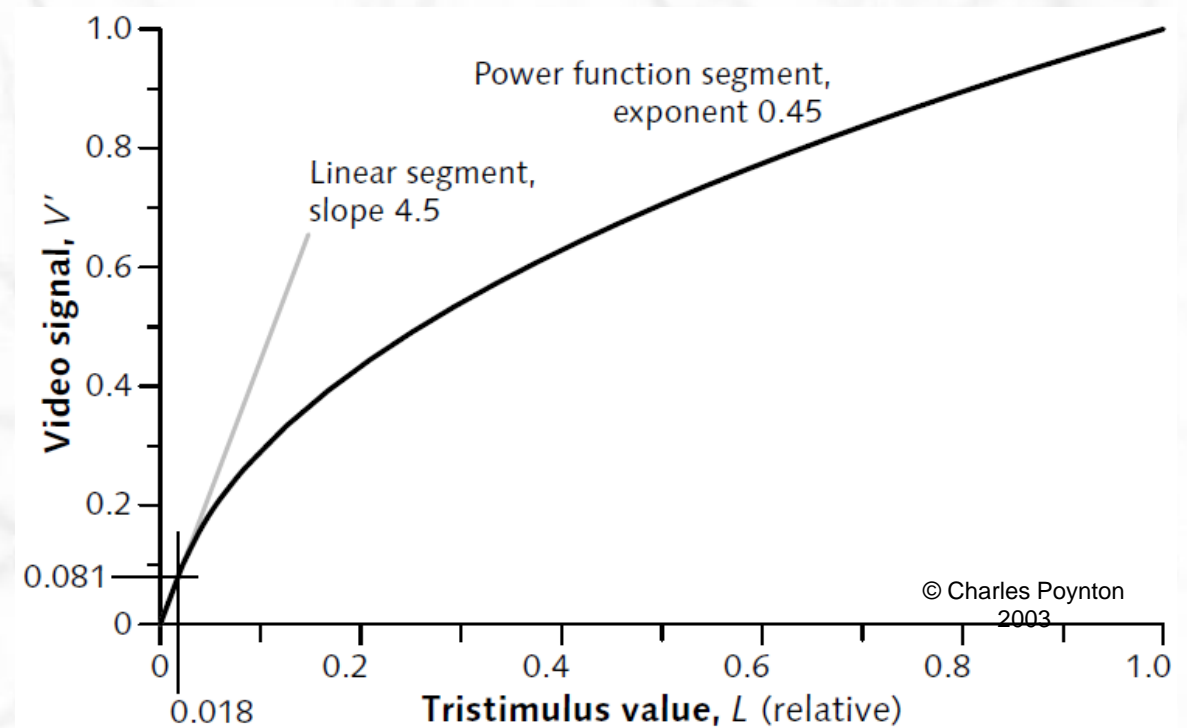
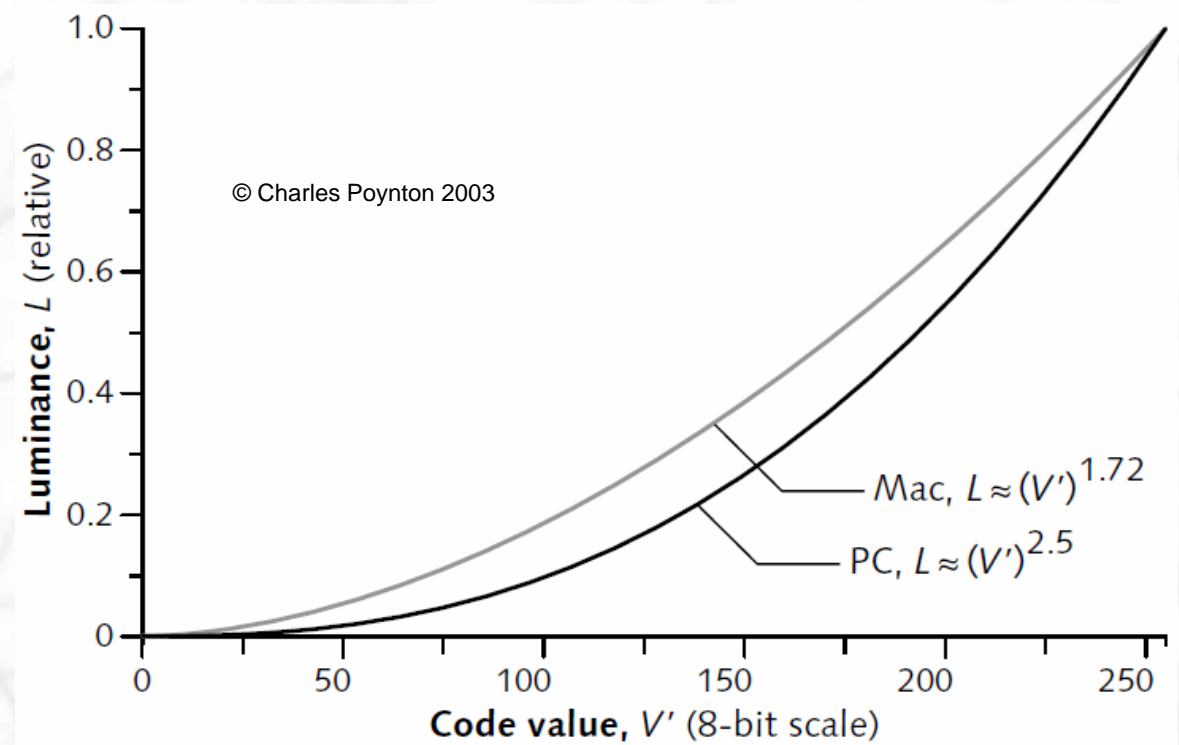
$$x \propto F^{1/\gamma} \text{ with } \gamma \approx 2.2$$

- Whereas in scientific image file formats (e.g., FITS), the recorded pixel values are proportional to the incoming flux:

$$x \propto F$$

- To help with convergence it is often appropriate to compress the dynamic range using e.g.,

$$x = \operatorname{arcsinh} \left(\frac{F}{\sigma_F} \right)$$



Photometric redshifts

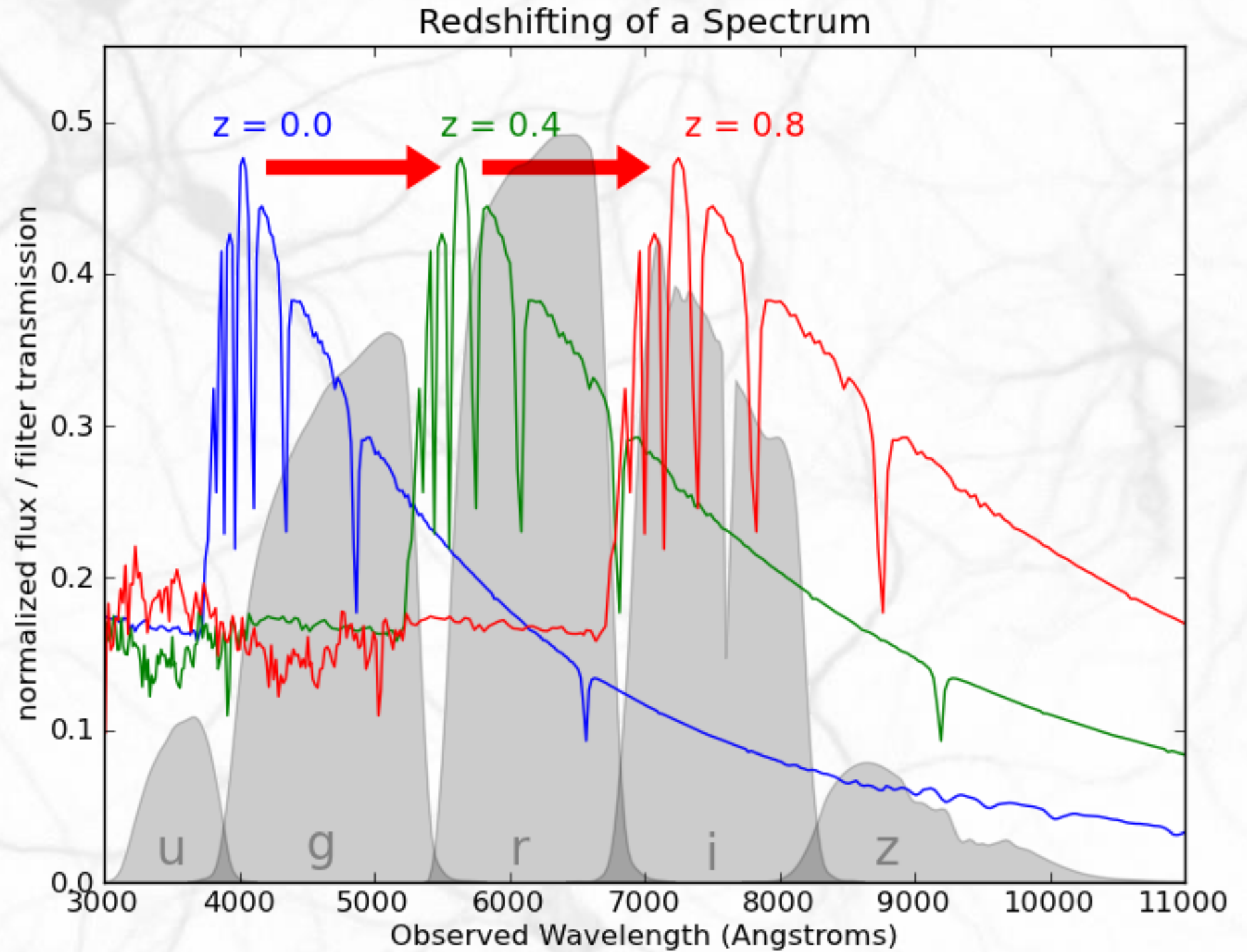
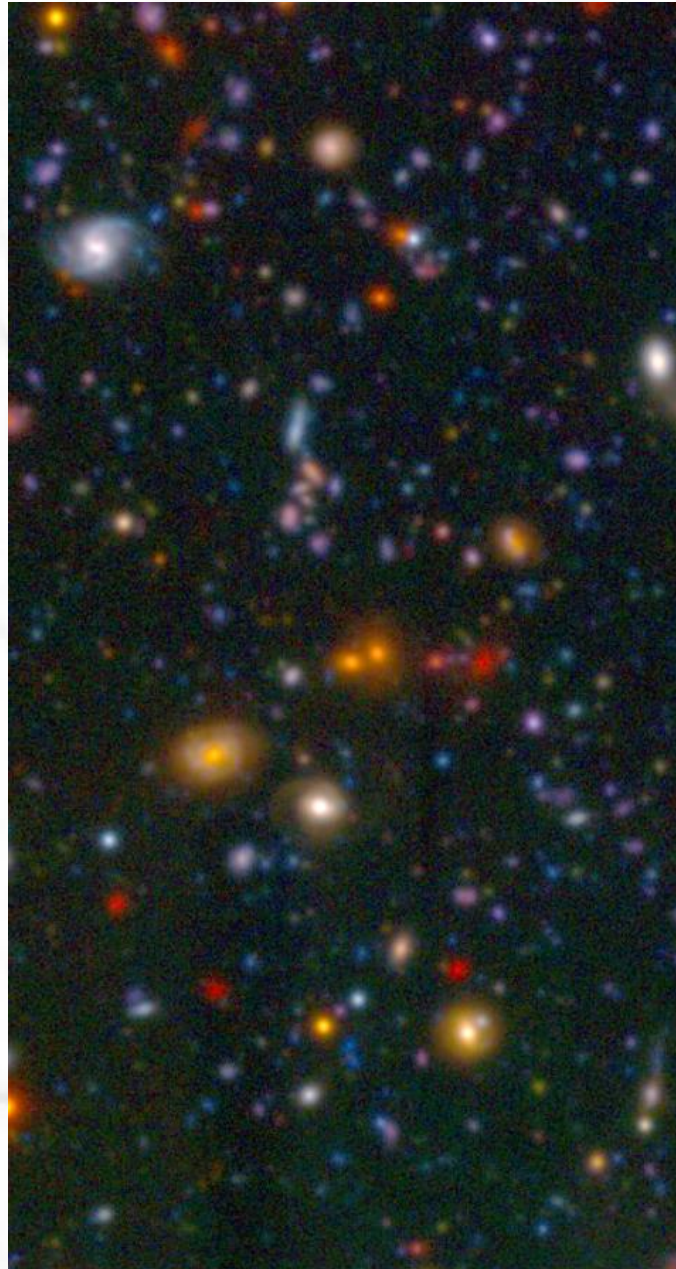


Photo-Z's using a CNN

J. Pasquet, EB, M. Treyer, S. Arnouts, D.Fouchez (**Pasquet et al. 2018**)

github.com/jpasquet/Photoz

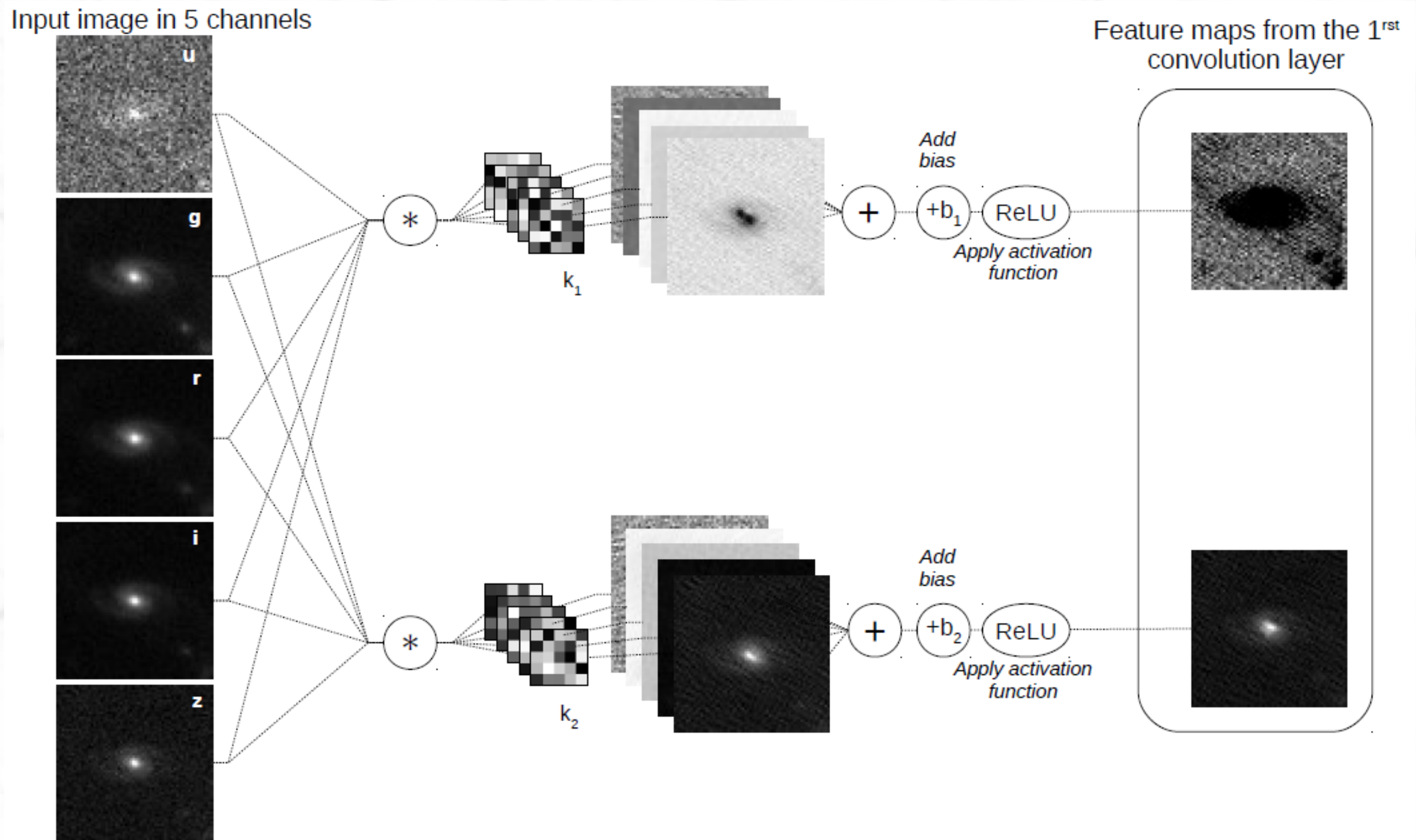


Photo-Z's using a CNN: Inception architecture

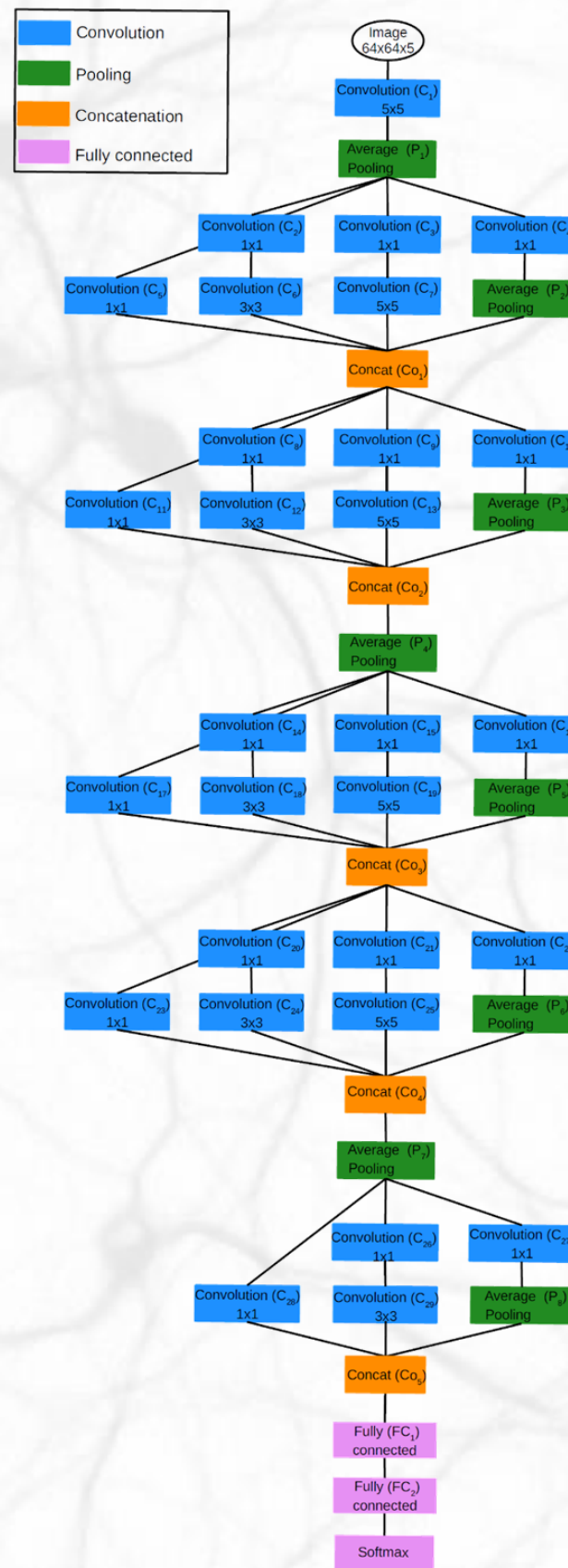


Photo-Z's using a CNN: results

Low z

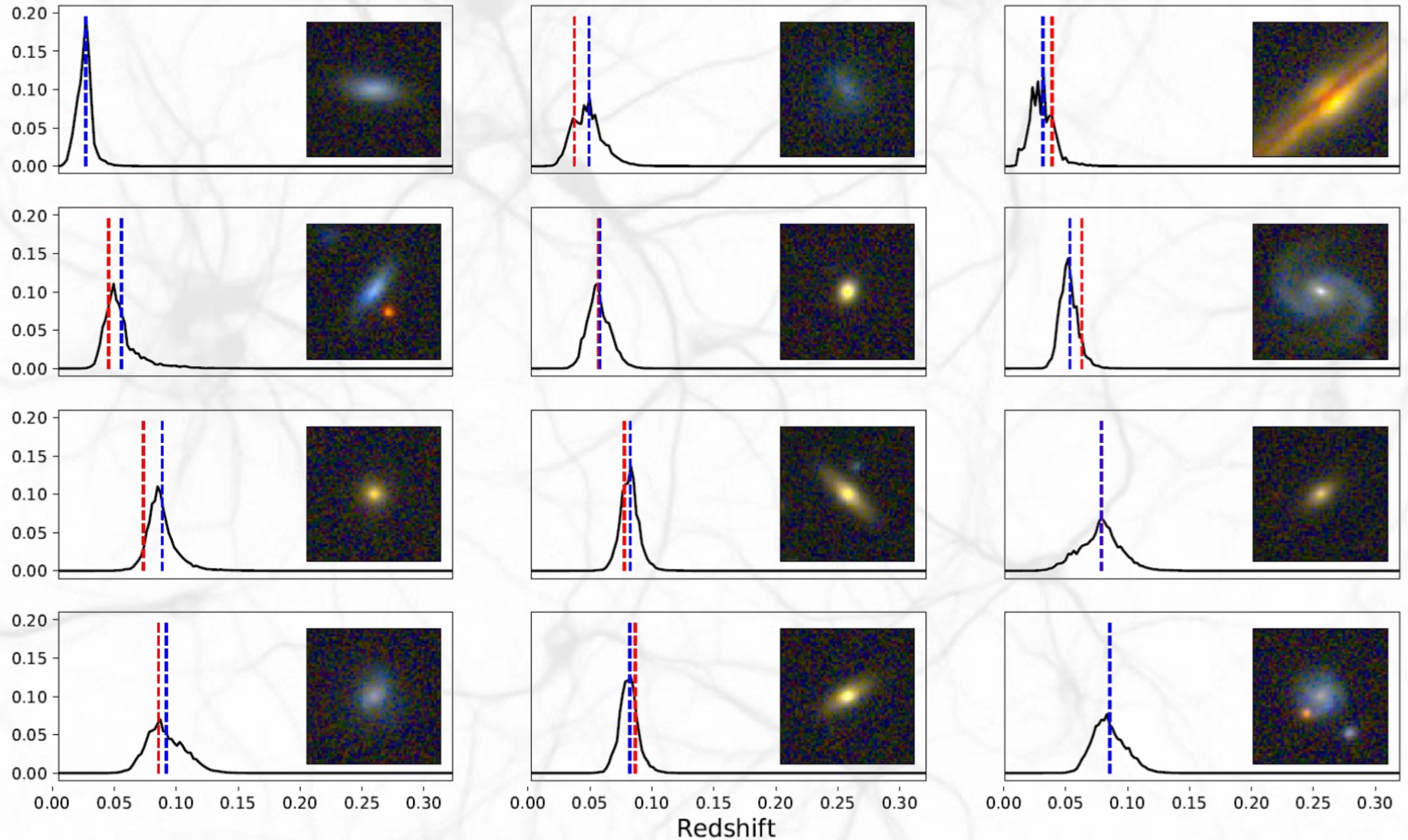


Photo-Z's using CNNs: results (cont)

High z

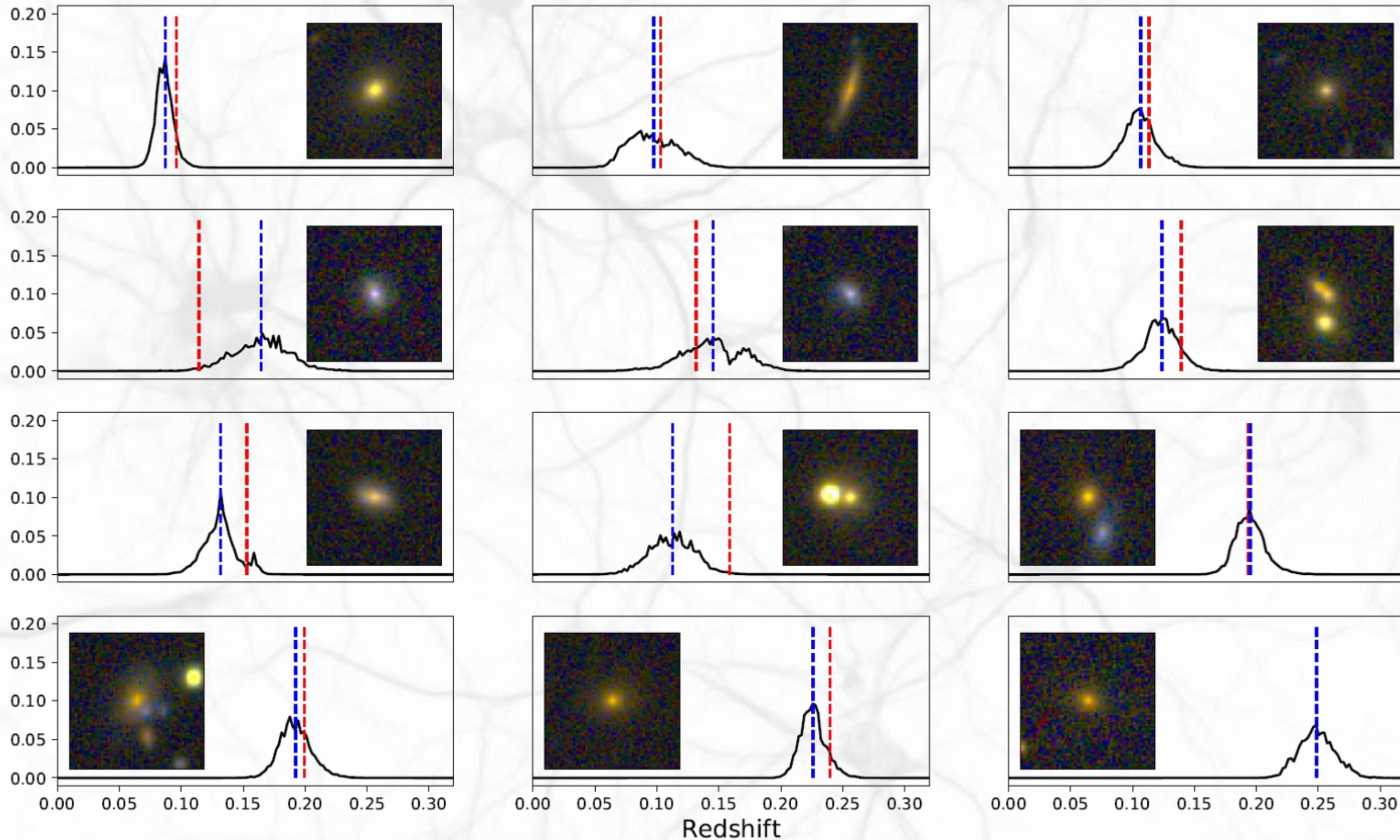


Photo-Z's using CNNs: results (cont.)

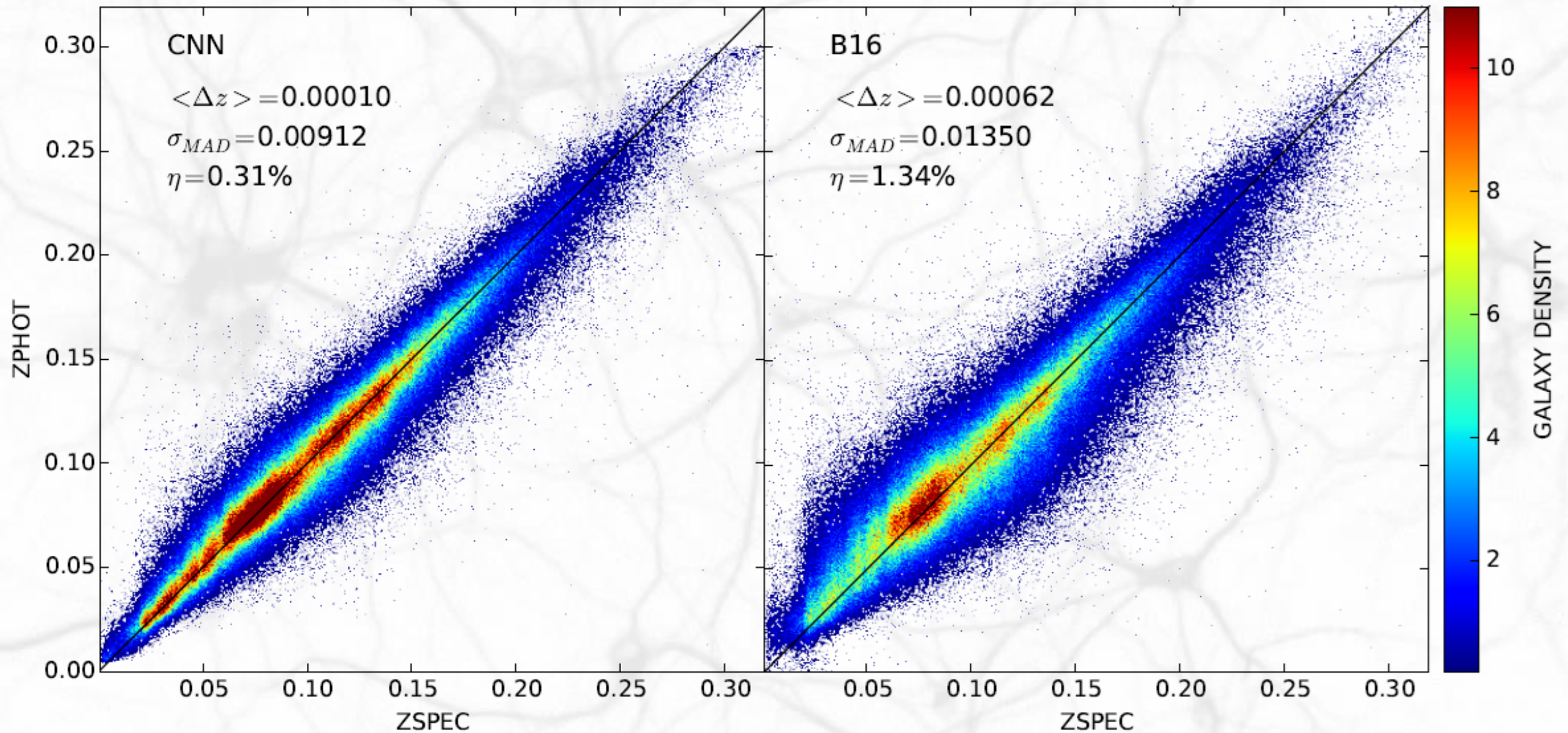


Photo-Z's using CNNs: effect of neighbors

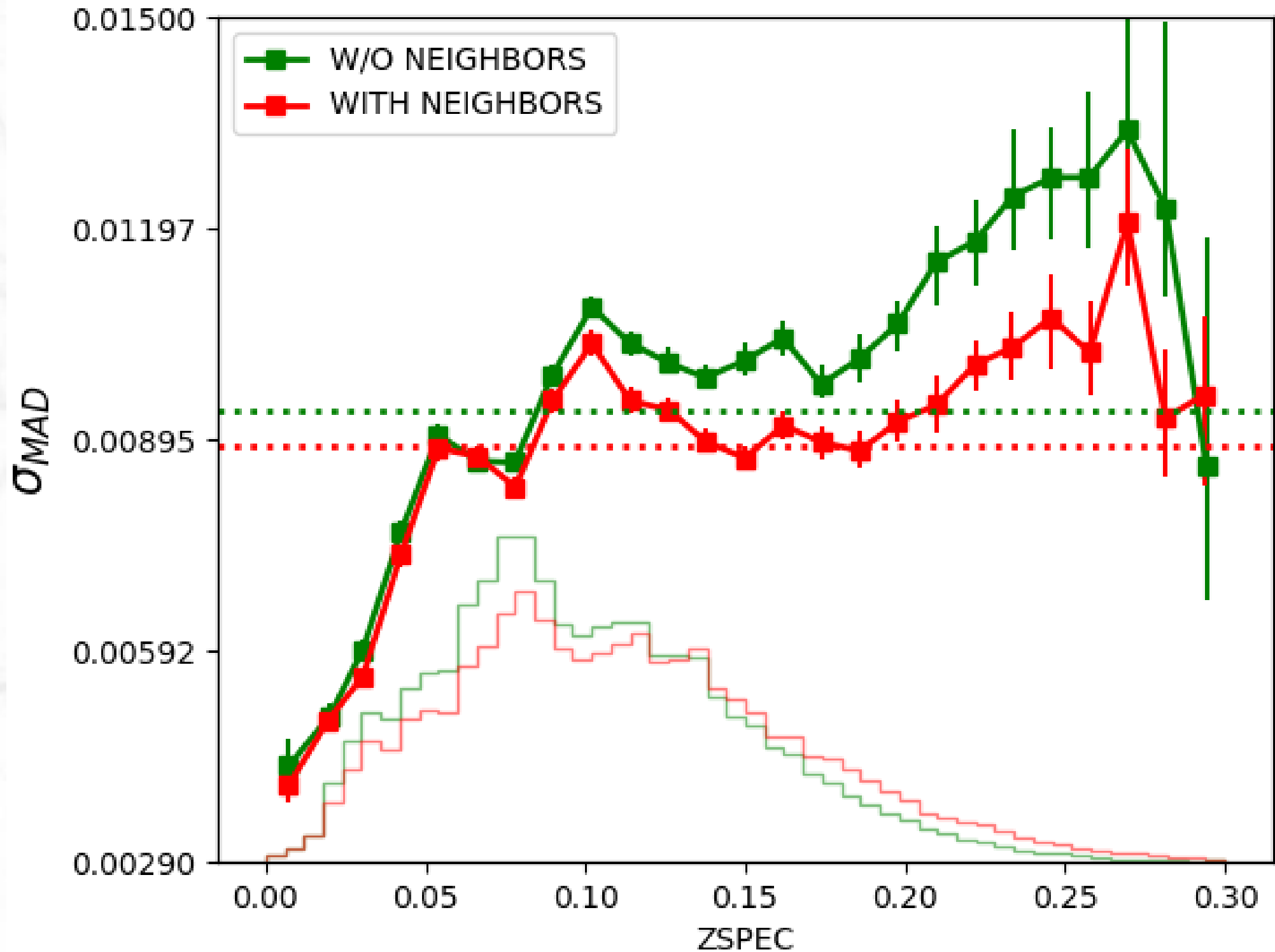


Photo-Z's using CNNs: biases (cont.)

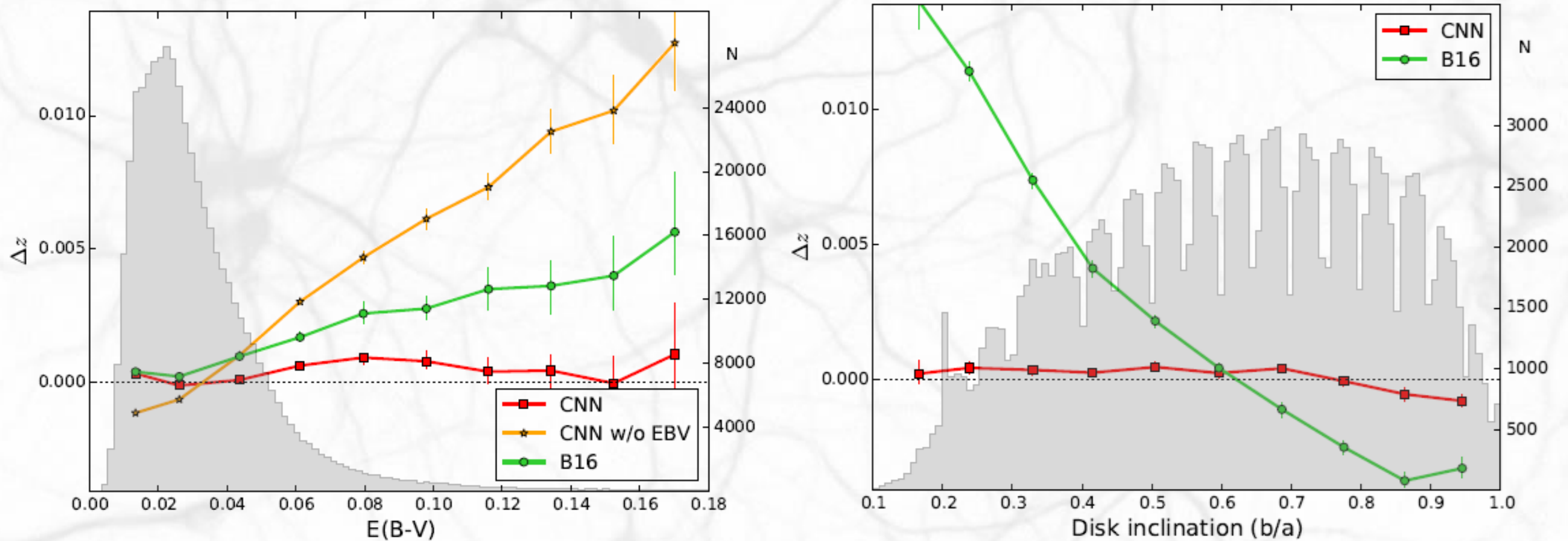


Photo-Z's using CNNs: dispersion

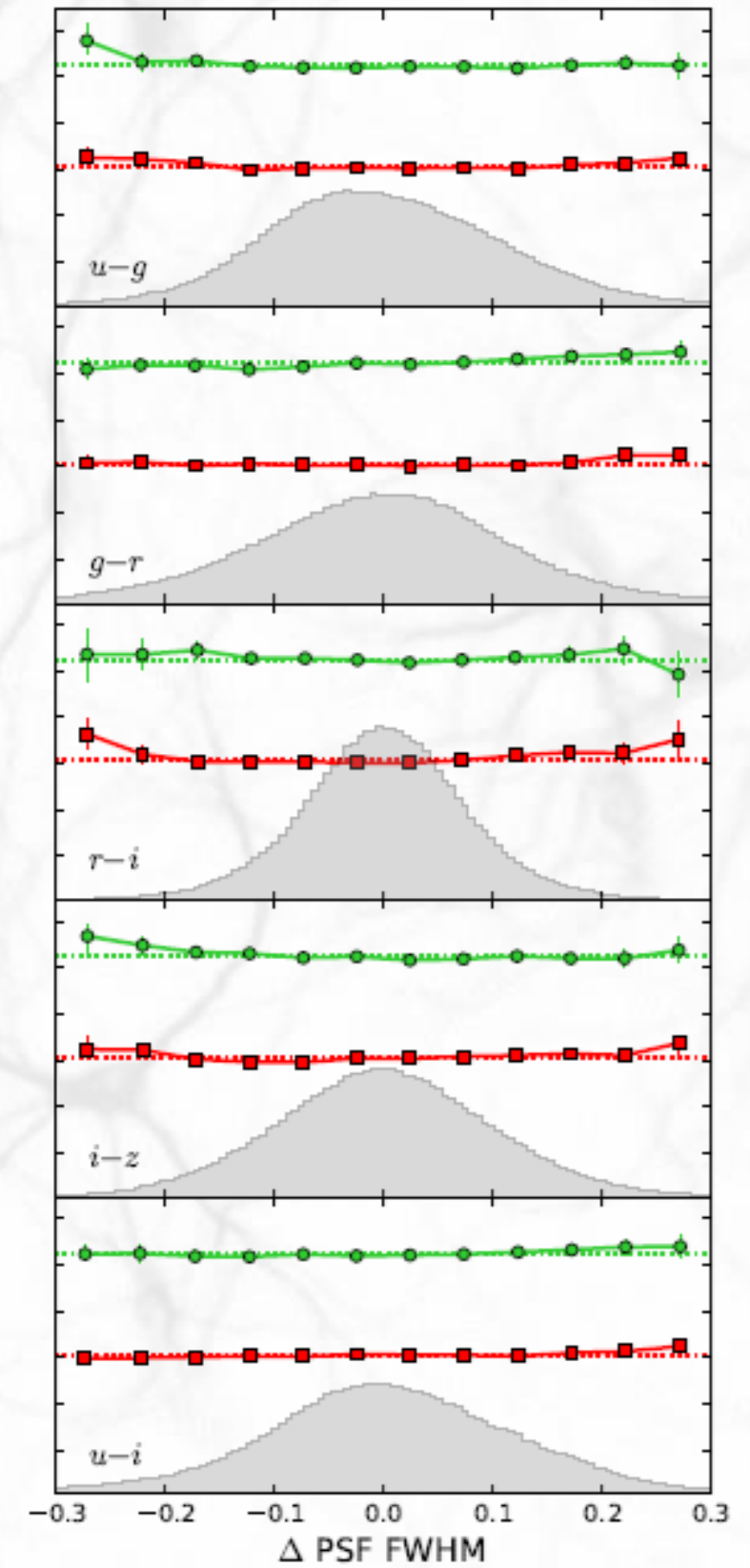
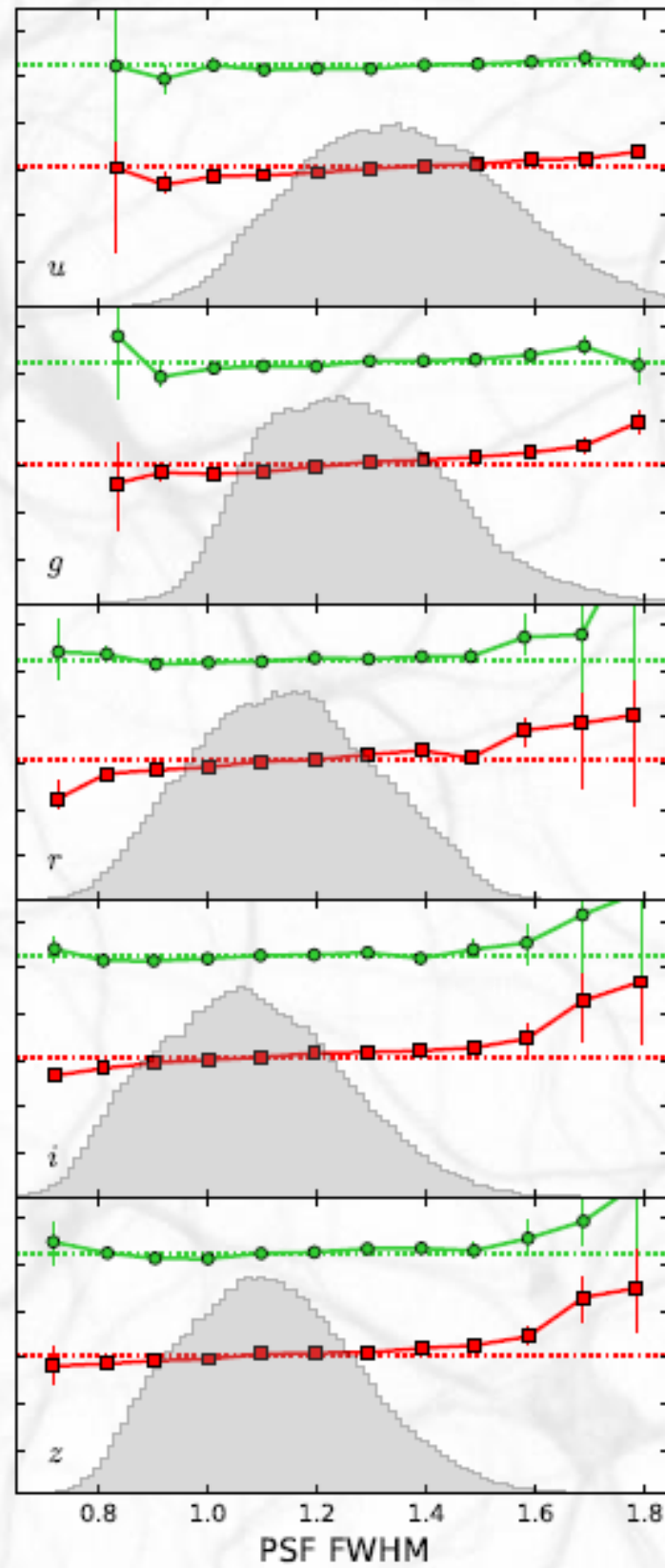
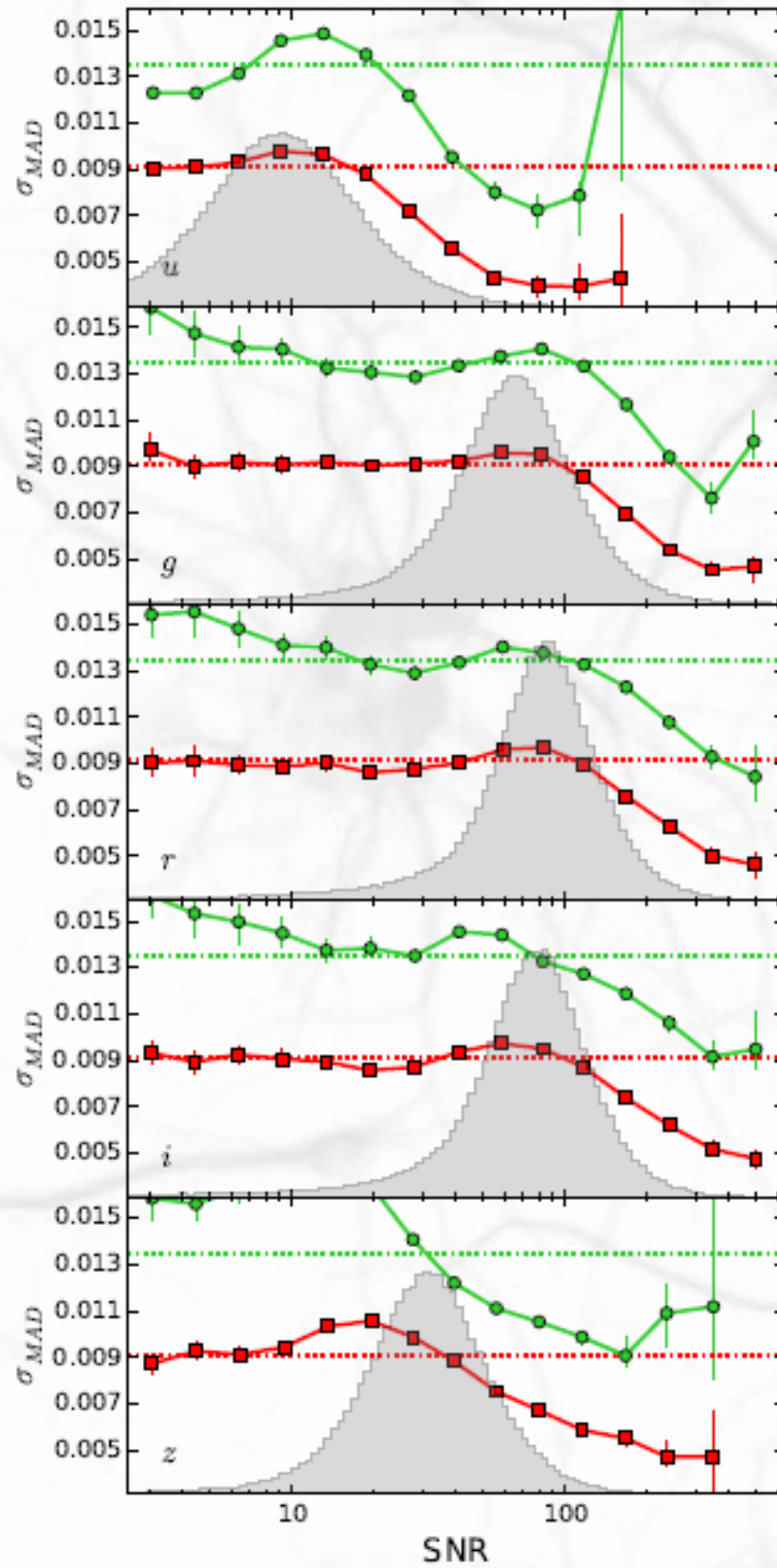
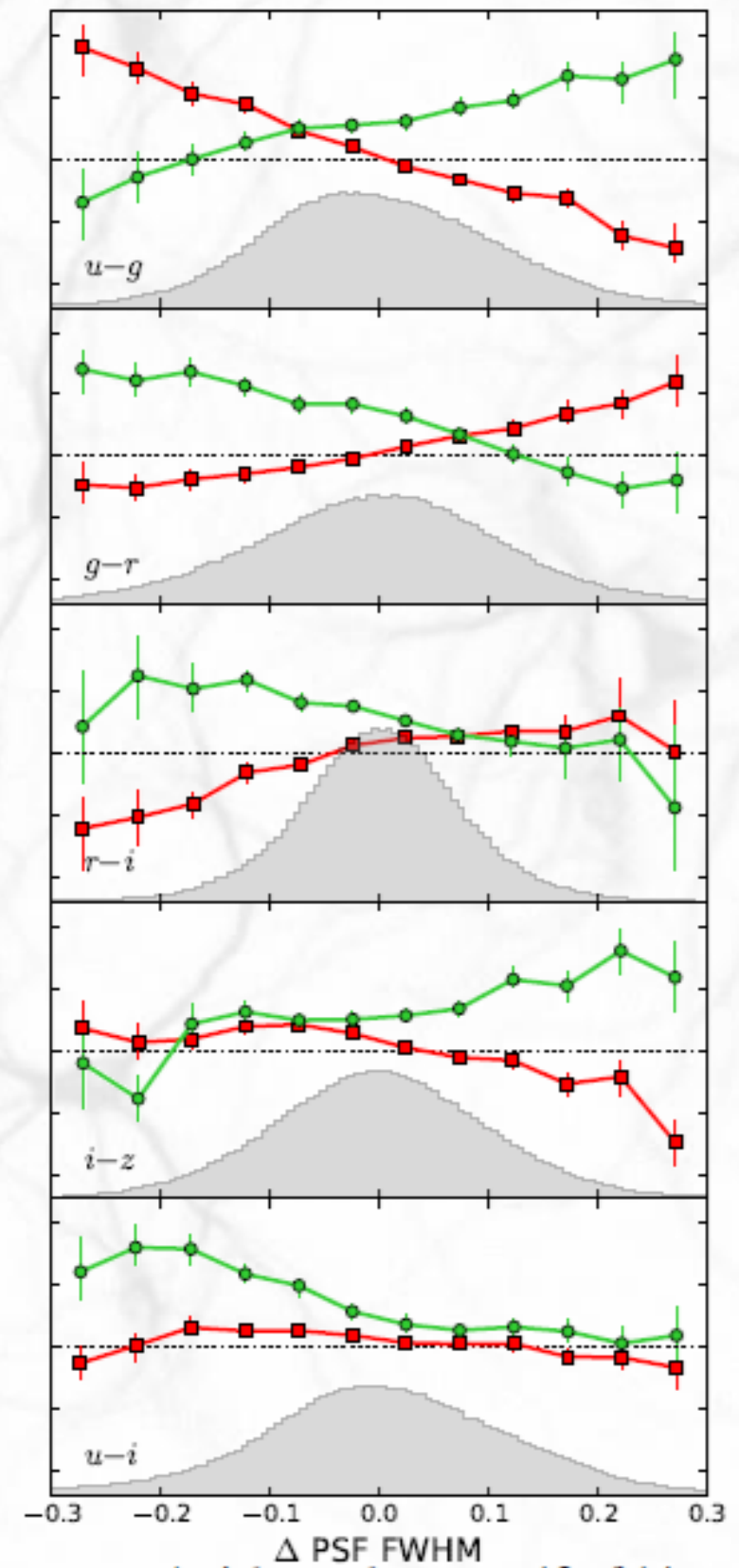
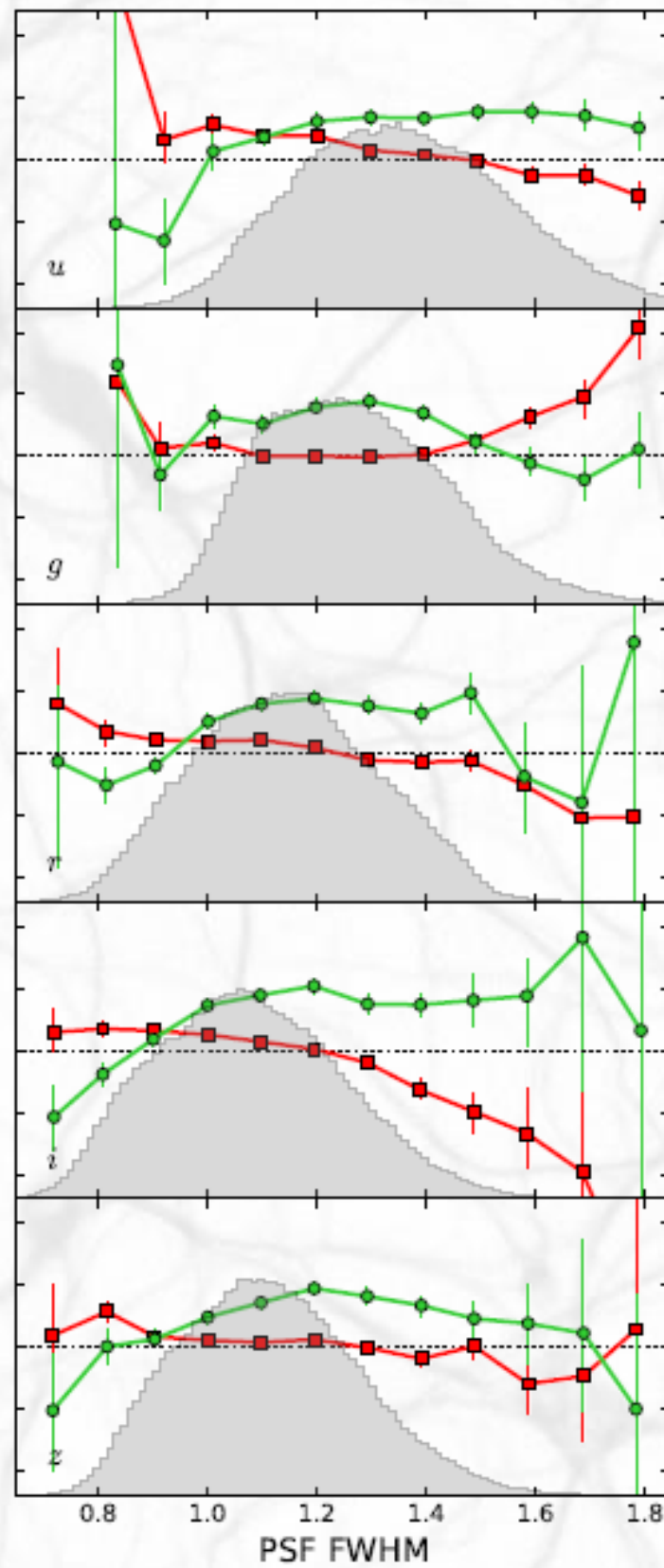
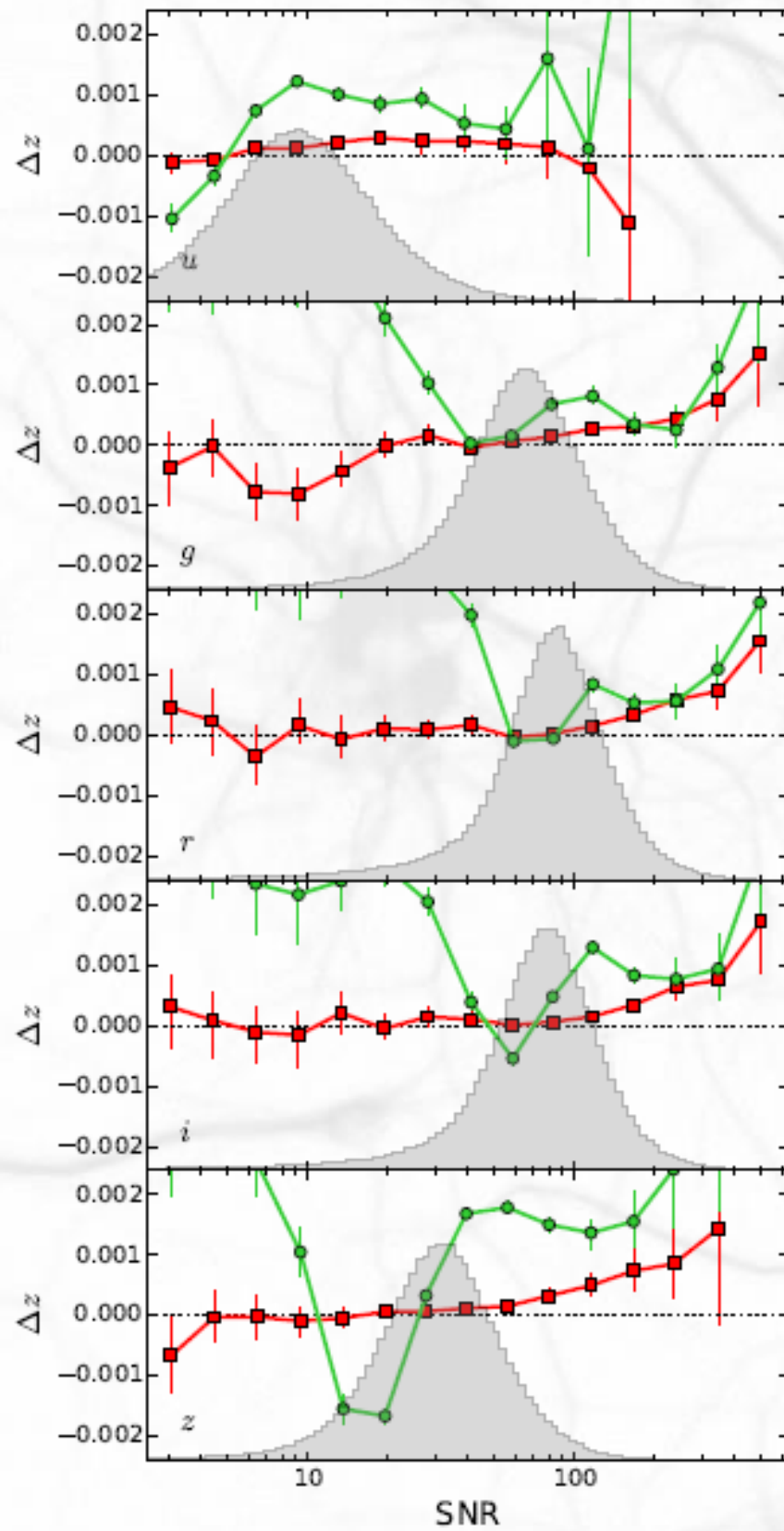


Photo-Z's using CNNs: biases (cont.)

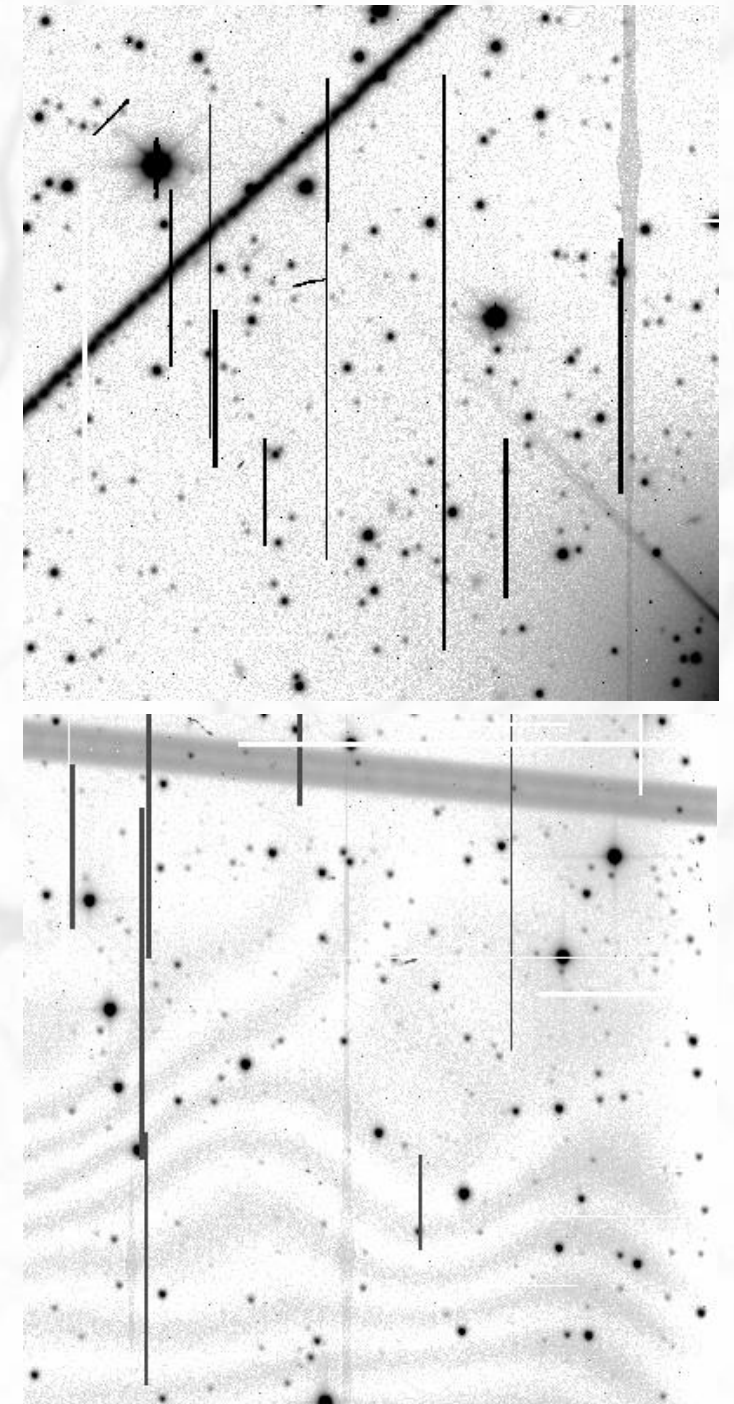


Detection of defects in astronomical images

M.Paillassa, EB, H.Bouy (**Paillassa et al. 2019**)

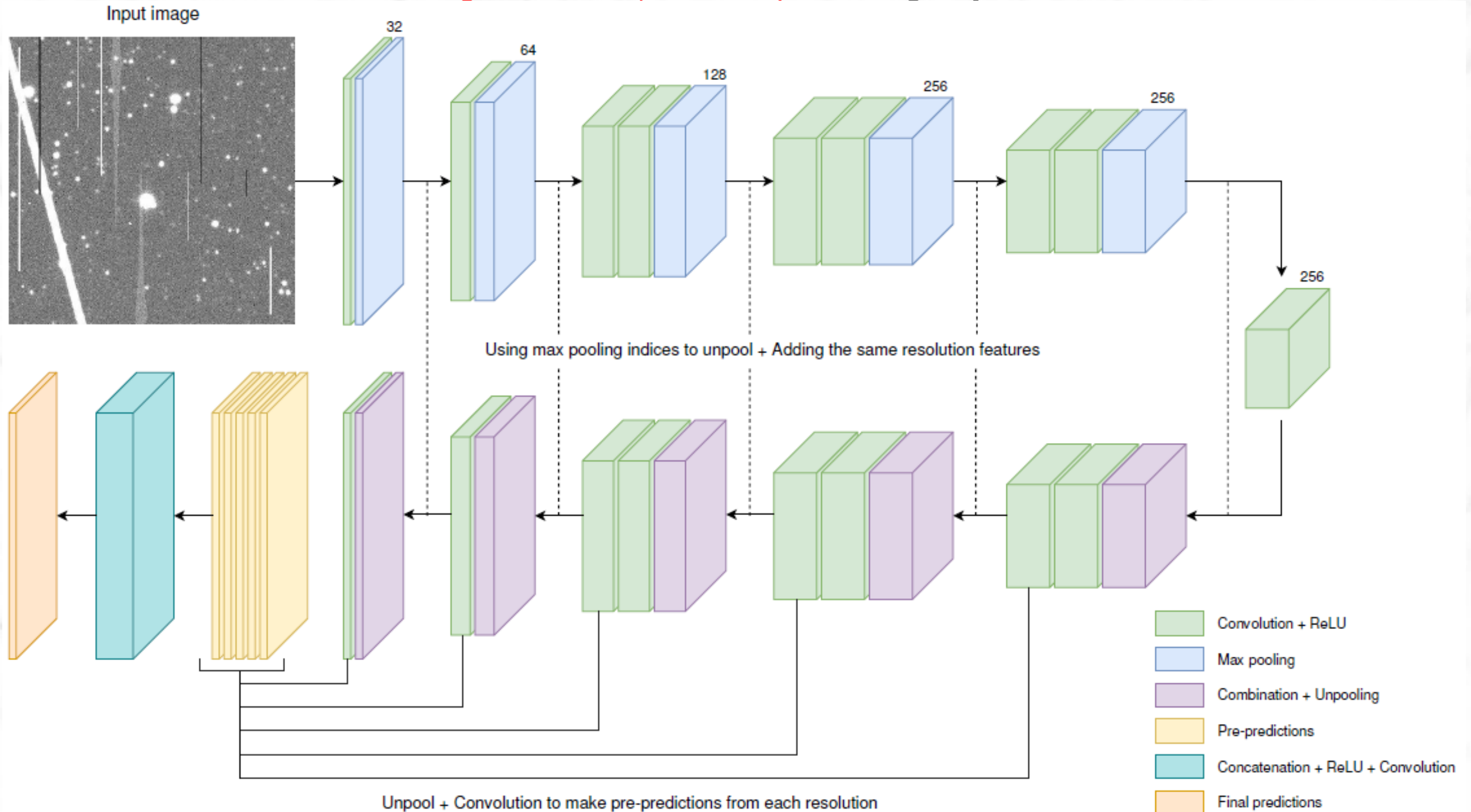
github.com/mpaillassa/MaxiMask

- Petabytes of astronomical image data now freely available online
 - Invaluable for studies of the variable sky
 - Inhomogeneous image quality
 - Many images hardly usable
 - Metadata often missing
- Efficient defect mapping/correction engine have been developed for large imaging survey pipelines
 - Highly tuned
- Here comes **MaxiMask!**

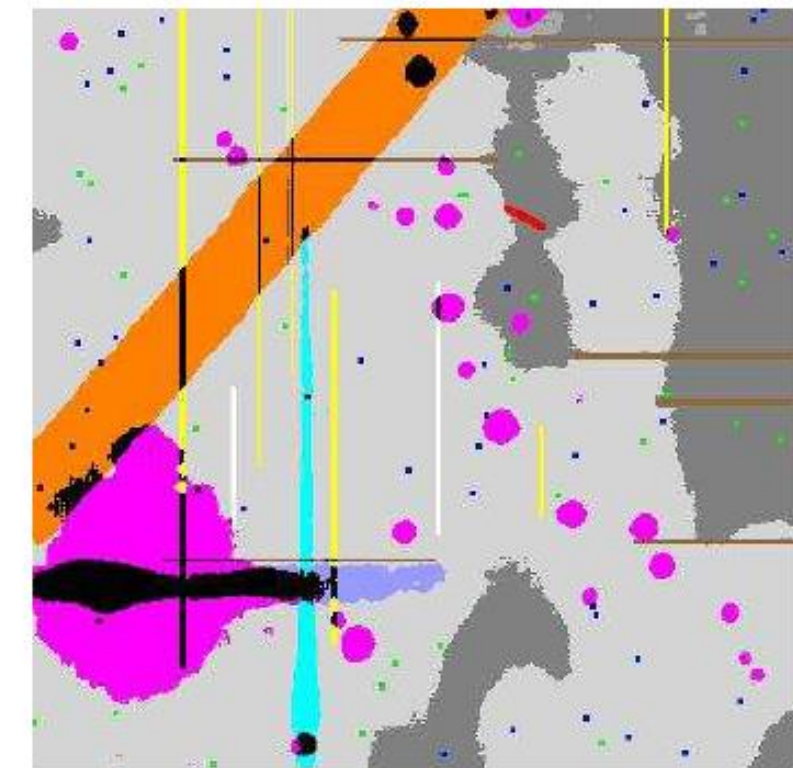
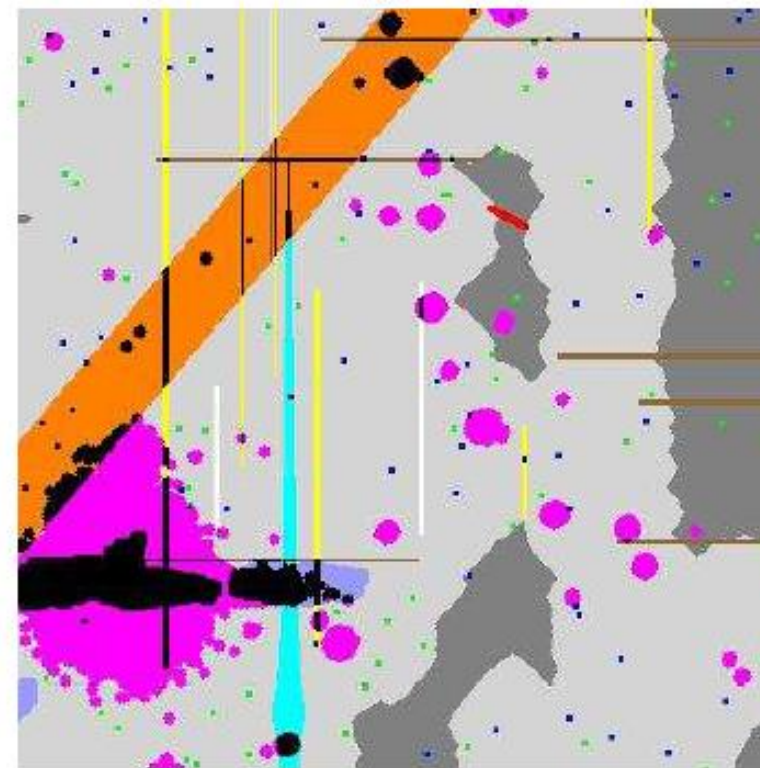
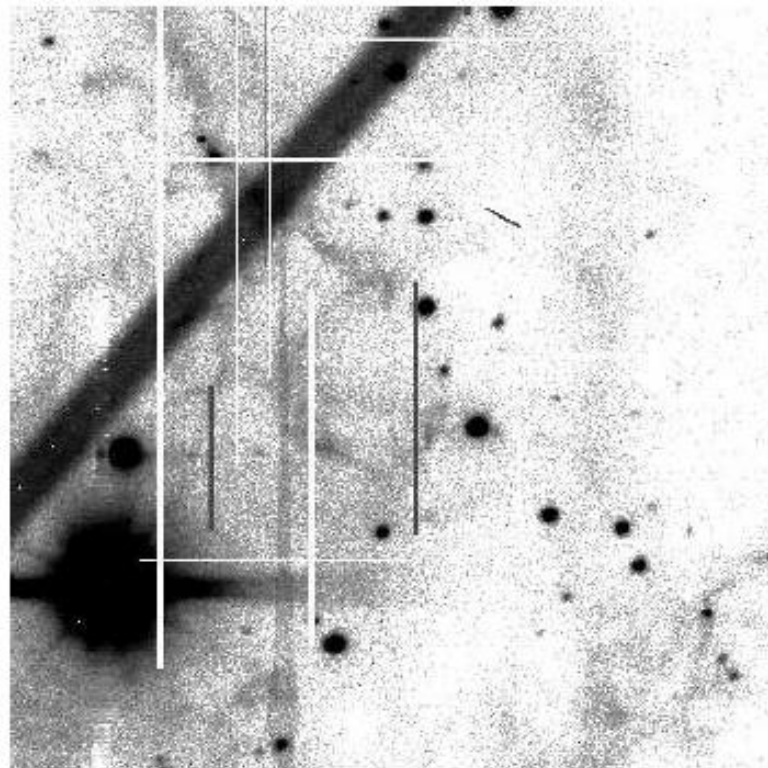
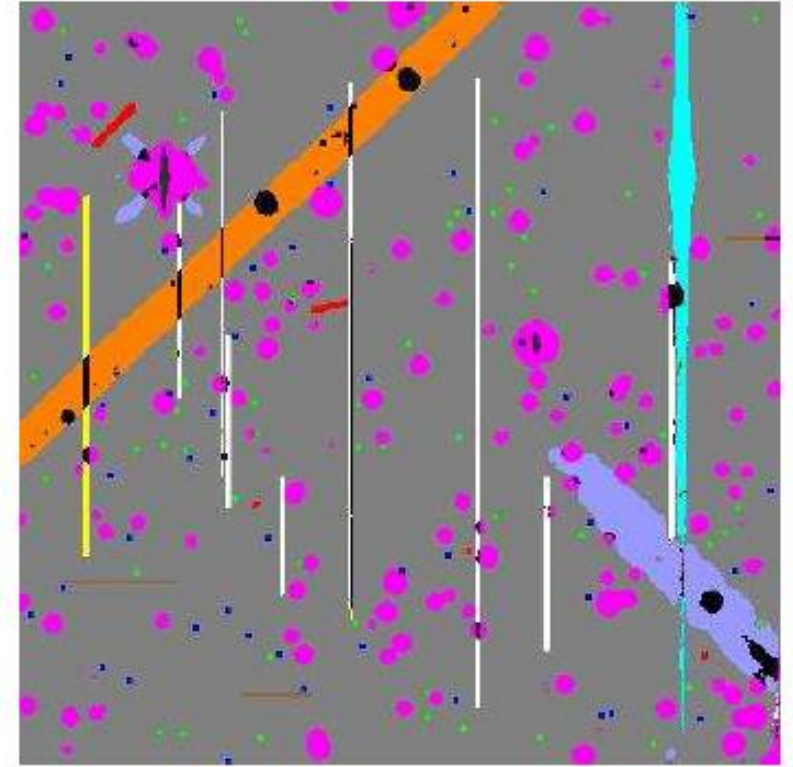
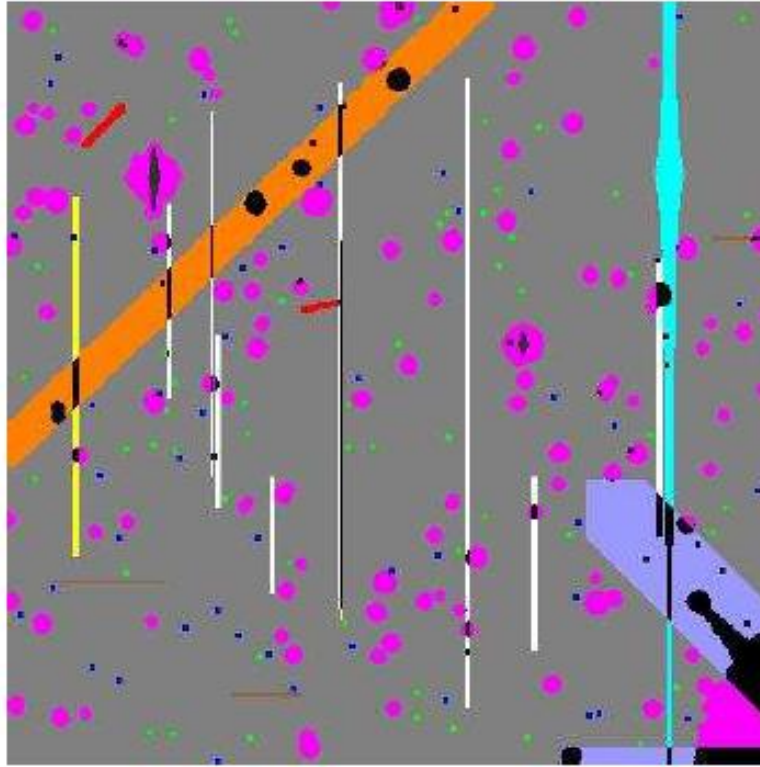
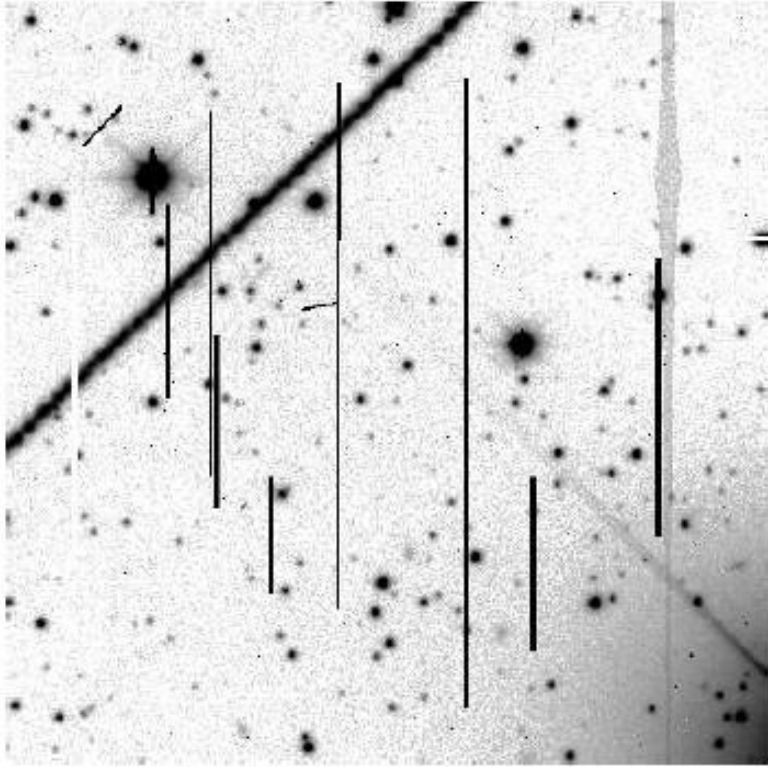


MaxiMask: architecture

- Derived from **Yang et al. (2018)** « Highly fused » model

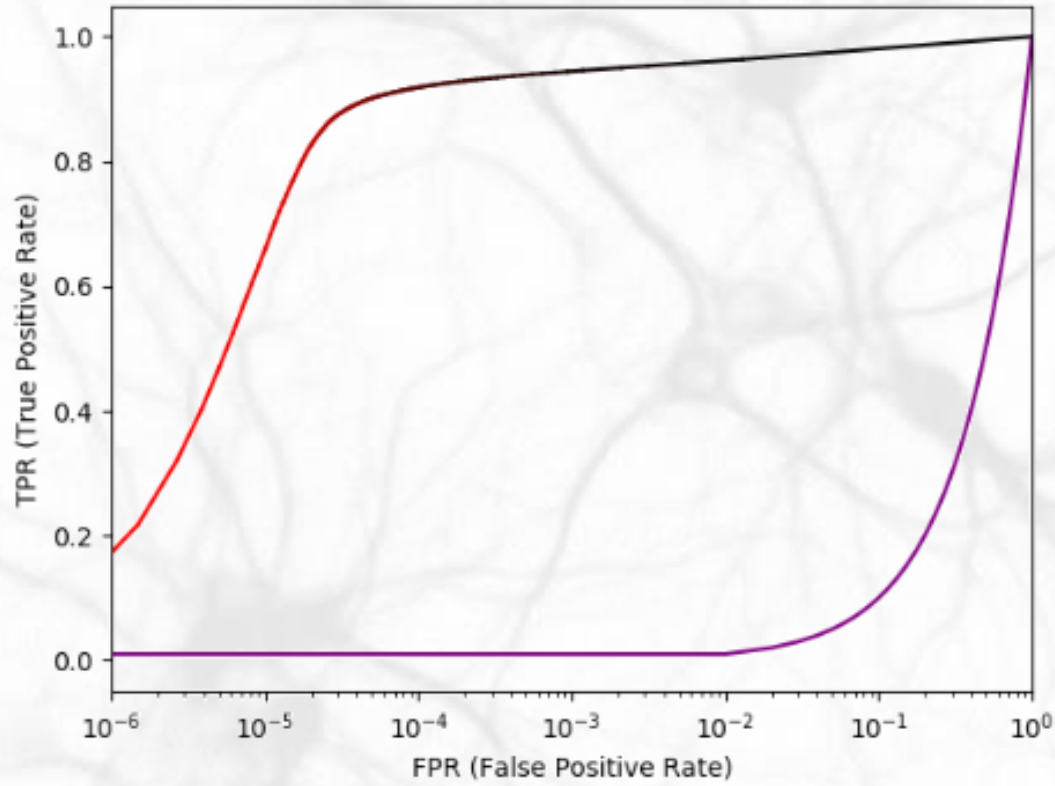


MaxiMask training

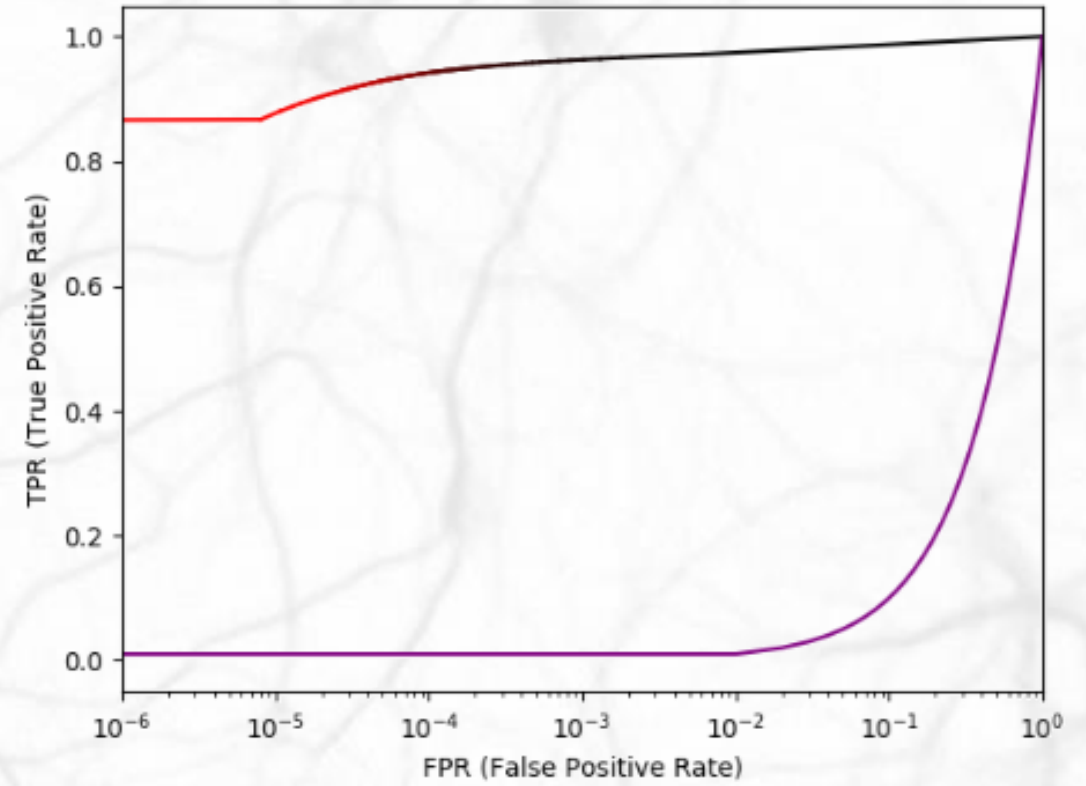


MaxiMask ROC curves

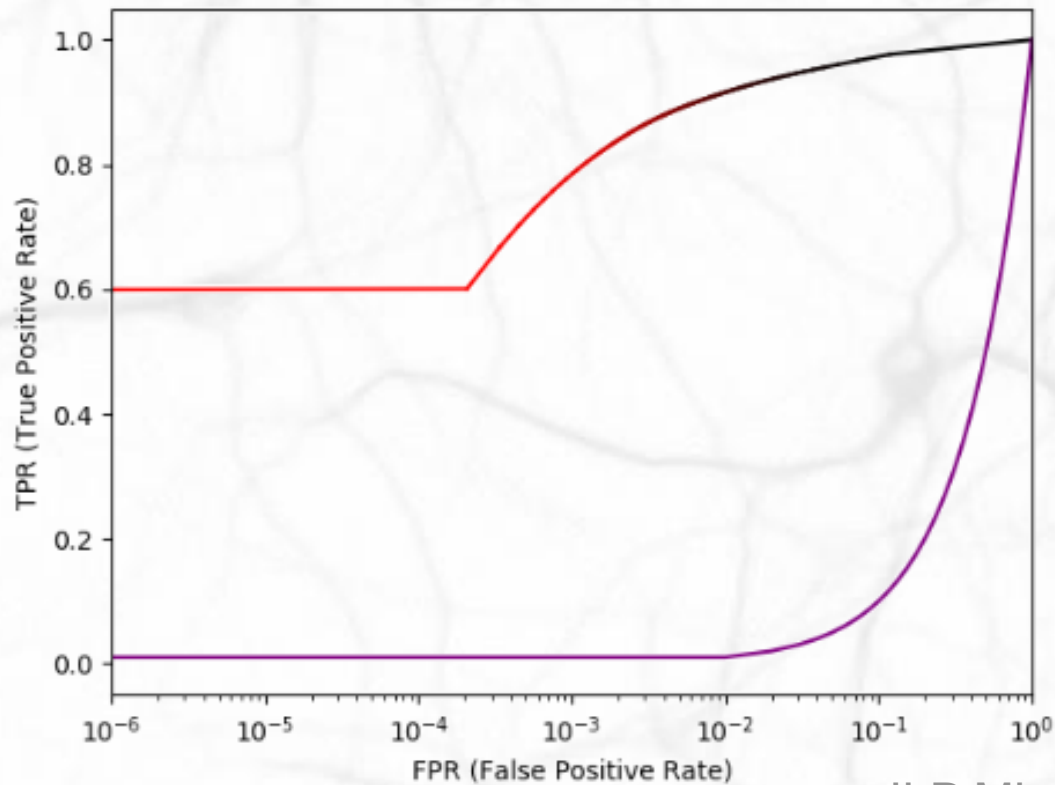
Hot pixels ROC curve
AUC: 0.98134



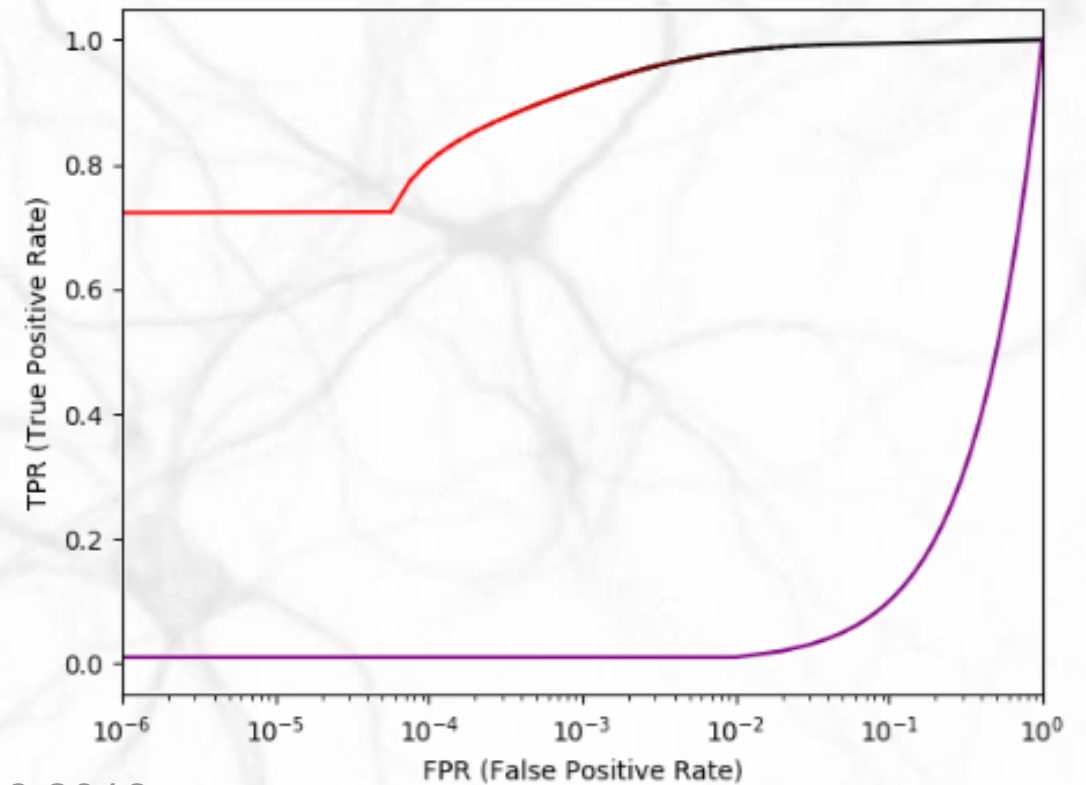
Bad pixels ROC curve
AUC: 0.98566



Persistence ROC curve
AUC: 0.98389



Satellite ROC curve
AUC: 0.99537



Conclusion

- The range of possible applications appears almost endless
- The classification performance of Deep CNN models significantly exceeds that of previous, state-of-the-art “traditional” astronomical image analysis algorithms
 - Working directly on pixel alleviates many difficulties
 - Properly trained models yields accurate PDFs
- Paradigm change in the way we process image data
 - Forward modeling all the way
 - Even “bigger data” than before
 - Knowledge of the physical and instrumental processes more useful than ever!